COMPARISON OF LOW-COST METHODS FOR VEGETATION MAPPING USING OBJECT BASED ANALYSIS OF UAV IMAGERY: A CASE STUDY FOR THE GREATER CÔA VALLEY, PORTUGAL

MEENAL SHARMA
August 2022

SUPERVISORS:
Dr. Panagiotis Nyktas
Dr. Francesco Nex

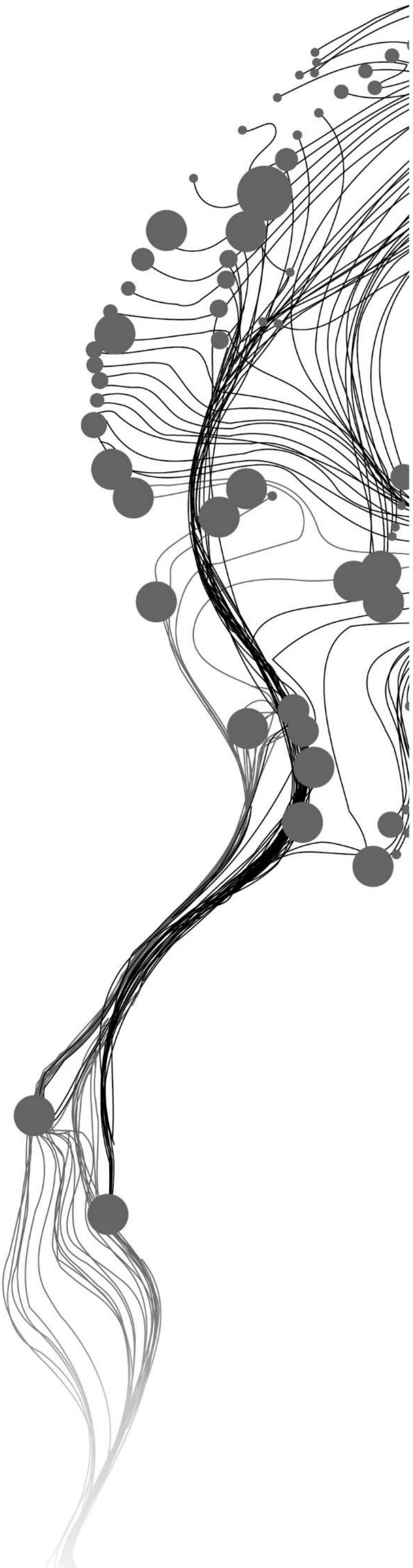

COMPARISON OF LOW-COST METHODS FOR VEGETATION MAPPING USING OBJECT BASED ANALYSIS OF UAV IMAGERY: A CASE STUDY FOR THE GREATER CÔA VALLEY, PORTUGAL

MEENAL SHARMA
Enschede, The Netherlands, August 2022

A thesis submitted to the Faculty of Geo-Information Science and Earth Observation of the University of Twente in partial fulfillment of the requirements for the degree of Master of Science in Geo-information Science and Earth Observation.

Specialization: Natural Resources Management

SUPERVISORS:
Dr. Panagiotis Nyktas
Dr. Francesco Nex

THESIS ASSESSMENT BOARD:
Dr. Tiejun Wang (Chair)
Dr. Chariton Kalaitzidis (External Examiner, Mediterranean Agronomic Institute of Chania, Crete, Greece)

ABSTRACT

Conservation planning for a highly diverse vegetated area and its ecosystem relies on accurate vegetation maps. Unmanned Aerial Vehicles (UAVs) have been proven reliable, efficient, and cost-effective tools in improving the monitoring of natural habitats and facilitating their management. UAV allows monitoring of remote and inaccessible areas through ultra-high resolution imagery. The conventional method of using ground survey is expensive and requires manual efforts, while UAVs with various advantages like cost-effective, flexible, and high spatial resolution can be used efficiently for mapping vegetation in a heterogeneous landscape. Using UAV high resolution images and Structure from Motion (SfM) processing, the research aims to assess the low-cost methods and the effectiveness of UAVs in vegetation mapping on the aspect of image compression, sensors, and seasonality. For UAV data acquisition, this research used the DJI-Phantom 4 RGB camera and Parrot Sequoia multispectral camera together at two sites in Greater Côa Valley, Portugal. The study examines the feasibility and potential of using SfM photogrammetry and object-based image analysis (OBIA) to classify vegetation into seven dominant life form classes. The workflow of OBIA consisted of segmentation and classification using Random Forest in eCognition software. The workflow was used to assess the efficiency of the methods in improving the classification accuracy of vegetation maps. Further, each classification results were compared using accuracy assessment i.e., overall accuracy and kappa value.

The study investigated the effect of image compression (raw DNG format and JPEG format) in vegetation classification, yielding a better classification accuracy in uncompressed RGB images (overall accuracy 80.65% and kappa 0.77) compared to compressed RGB images (overall accuracy 62.04% and kappa 0.54). Secondly, vegetation classification was compared between sensors, for which RGB camera and Parrot Sequoia multispectral camera were used to acquire RGB and multispectral images, respectively. The classification accuracy of different classes improved using multispectral images (overall accuracy 85.19% and kappa 0.83) compared to RGB images. The study also assesses the importance of Ground Control Points (GCPs) in vegetation mapping. Lastly, to determine the usefulness of seasonality in vegetation classification, single-season image classification was compared with tri-seasonal image classification. The outcome of vegetation classification for seasonal comparison showed that tri-seasonal images have higher accuracy in each life-form class than single-season images. The overall accuracy resulted in 92.99% and 0.91 kappa value for the orthomosaic of the combination of three seasons images. The results from the study show that SfM processing with OBIA is a useful method for vegetation classification, and OBIA is sensitive to the number of training samples used for image classification. It is also found that multispectral sensor is useful in identifying different life-form, but the combination of seasonal image classification (using RGB images) has resulted in the best overall classification accuracy. However, GCPs are significant in aligning multi-temporal images and can be helpful for future monitoring purposes. From the study, these low-cost methods have shown potential in classifying vegetation precisely, but processing requires high computational storage. The study elaborates that these accurate vegetation maps can be used to monitor vegetation changes for the factors such as the introduction and increase of herbivores and grazing in the area. The present research results offer valuable information for optimizing a UAV-based vegetation mapping protocol to be used in all Rewilding areas in Europe and other conservation areas.

Keywords: UAV, Vegetation mapping, Object-based Image Analysis (OBIA), Structure from Motion (SfM), random forest

ACKNOWLEDGEMENTS

I want to express my heartfelt gratitude to my first and second supervisors, Dr. Panagiotis Nyktas and Dr. Francesco Nex, for their constant motivation, guidance, and constructive feedback throughout my research. The valuable discussions and suggestions during these last months enabled me to complete my study.

I want to thank my chair, Dr. Teijun Wang, for his critical evaluation, comments, and suggestions during the research proposal and mid-term defense, which contributed to the quality of my research. I want to thank Dr. Chariton Kalaitzidis for his time and feedback on improving the thesis.

I would also want to extend my thanks to Drs. R.G.Nijmeijer, NRM course director for coordinating MSc research proceedings and all the guidance during the fieldwork required. I am also thankful to all the NRM staff who taught us and shared their knowledge and experiences during their courses; I learned a lot from each of you.

I sincerely thank the drone pilot and my first supervisor, Dr. P. Nyktas, who accompanied me and helped collect the UAV data, guided me during fieldwork, and made all necessary arrangements for the field trip to Portugal. I want to thank Mr. T.M.R. Roberts and Mrs. Camilla Marcatelli for helping in arranging all essential types of equipment for the fieldwork and for training how to use differential GNSS in the field.

I want to offer my sincere thanks to the team of Rewilding Portugal in Guarda for granting us permission to fly drones and collect the data from different plots. I am highly grateful to Mrs. Sara Aliácar and Mr. Andre Couto for assisting us during the field trip and organizing the necessary arrangements for our stay in Vale de Madeira. The motivation for their work and the knowledge they shared about the Côa Valley was inspiring and valuable for me and my research.

A sincere thanks to Student Affairs personnel for always being available and assisting me whenever I needed their help; their love and concern for the students have made our journey easy. At the same time, I would like to extend my sincere thanks to ITC for awarding me the ITC Excellence Scholarship, which helped me pursue this course and provided all the necessary resources for completing my degree.

Finally, my deepest gratitude to my family and friends for always being there with me, supporting me in each stage of my life, and always motivating and encouraging me during my lows. This journey was not a smooth sail, but we all made it to the end. I was blessed, and for this, I will thank God for keeping me healthy and giving me the strength to go through the challenging situation.

Thank you.

Meenal Sharma

August 2022

TABLE OF CONTENTS

LIST OF FIGURES

LIST OF TABLES

1. INTRODUCTION

1.1. Background and justification

Vegetation is an integral feature of every landscape that helps regulate water, nitrogen, and carbon biogeochemical cycles as well as regulate climate and support biodiversity. Vegetation patterns respond to the region's environmental conditions and historical factors like natural disturbances, soil properties, land-use history, etc. (Motzkin et al., 1999). Many critical plants and their communities are at risk of habitat loss (Müllerová et al., 2017), and plant conservation plays a vital role in achieving Sustainable Development Goals (SDGs) (Sharrock and Jackson, 2017). In general terms, plant conservation contributes directly or indirectly to all 17 Sustainable Development Goals (SDGs). However, it has a specific contribution to individual targets under particular goals (like target 6.6 protect and restore water-related ecosystems, target 12.2 sustainable management and use of natural resources, target 14.2 protect and restore ecosystems, target 15.5 protect biodiversity and natural habitats and many more (Sharrock and Jackson, 2017).

People have used several materials and methods to monitor, manage, and conserve the protected areas (Heywood and Iriondo, 2003), necessitating time and effort to survey and map the area, making it costly. Using aerial photographs coupled with substantial fieldwork to record the data requires experience, and vegetation classification and mapping is a prerequisite for natural resources inventory, land-use planning, and forming a baseline to monitor the changes in the landscape. Vegetation mapping is done to understand a region's vegetation patterns, in which factors such as the scale of an area, the source of data, the type of information, and the method are considered. Traditional methods such as literature review, map interpretation, ancillary data, and field survey are important for mapping vegetation, but they are time-consuming, expensive, and laborious (Xie et al., 2008). Vegetation mapping using aerial images acquired by manned aerial photography and fieldwork used to be difficult for the experts to analyze the area in minimum time (Morgan et al., 2010). Using aerial photos to monitor minor changes and differentiate vegetation change was difficult in large areas without any field reference.

However, digital image classification using satellite imagery of large areas effectively classified different vegetation (Baxendale et al., 2016). A survey was usually considered the primary method of mapping the vegetation, but for large inaccessible areas, satellite imageries are mainly used with remote sensing techniques to discriminate the plants on the community level. With the advancement in technology, different sources of remote sensing imageries are available, like Advanced Very High-Resolution Radiometer (AVHRR), SPOT-4, MODIS, etc., which can be classified, analyzed, and compared for various use. Each source of images can be used for vegetation mapping with different spectral, spatial, radiometric, and temporal characteristics (Xie et al., 2008).

Satellite imagery is used in classifying the land cover, but sometimes it lacks precise information for vegetation mapping due to low-resolution images (Berra et al., 2019). Unmanned Aerial Vehicle (UAV) can assist in surveying and characterizing plant species in very high spatial resolution data at a low cost (Müllerová et al., 2017). Unlike traditional field observations, drone imagery has a superior level of detail that can identify individual plant species for areas larger than the size of quadrats (Baena et al., 2017). On the other hand, satellite data is less efficient in detecting vegetation differences based on their phenology than UAV images due to coarse spatial resolution (Strong et al., 2017). The distinct advantage of using a UAV (with a digital camera) over conventional pilot aircraft and satellites is its low cost, better spatial and temporal resolution with operational flexibility to produce orthoimages, and Digital Surface Model (DSM) (Agüera-Vega et al., 2017a).

UAV has gained significance for capturing images for qualitative research for precision agriculture, cartography, forest management, marine conservation, and quantitative remote sensing applications (Radoglou-Grammatikis et al., 2020; Crommelinck et al., 2017; Manfreda et al., 2018; Johnston, 2019; Aasen et al., 2018). UAV can be an efficient method for mapping the vegetation precisely and creating detailed vegetation maps (Kaneko and Nohara, 2014), which can be used to gain information about the region. The constraints of poor weather conditions and cloud cover should be considered before a UAV flight. Studies on the plant species are frequently conducted at the local scale with help from UAV mapping and satellite remote sensing (Kattenborn et al., 2019). The combination of satellite data (Sentinel-2 and Pleiades) with UAV have been demonstrated to be useful for habitat mapping in wetland region using a spectral unmixing approach and can fill the gap between in-situ survey and satellite imagery with some technical limitations (Alvarez-Vanhard et al., 2020). A study by Kattenborn et al., (2019) proposed using UAVs instead of ground surveys because of better species identification as UAVs can discriminate plant communities on a scale of 1/50. Another by Baena et al., (2017) suggests that UAVs can be an excellent alternative to satellites to obtain color and infrared imagery for an affordable price. By providing high-resolution images and determining plant development over time, drones could contribute to in situ conservation of highly endangered plants (López and Mulero-Pázmány, 2019; Räsänen and Virtanen, 2019).

When it comes to ultra-high resolution UAV data, it is crucial to have a thorough understanding and familiarity with UAV technology, particularly the communication method between the drone and the imaging equipment. Images captured and obtained from UAV photogrammetry platforms generally come in different formats. These formats of the images depend upon the compression methods. The term compression refers to the method that helps reduce the amount of the data, whereas the data signify a certain amount of information. The image compression in UAV photogrammetry is performed mainly in two different ways, a) loseless and b)lossy. The process of lossy and loseless depends upon the compression scheme, which may lead to a decrease in image quality, information, and size. In image processing methods, the various image formats adapt different compression schemes, such as the most common image format, "TIFF" which uses a loseless method. In contrast, another popular format called "JPEG" utilizes controllable losses (Alfio et al., 2020). JPEG files lose some potential information but are easy to store and can be used directly on various electronic devices compared to RAW format images. However, RAW files are best suited to the detailed identification of plant parts. It is because RAW images have a greater range of color values than other formats (Sharma, 2019).

It is difficult to obtain the accurate spatial distribution of highly heterogeneous plant communities using traditional field methods and remote sensing, which led to using UAVs with multispectral sensors to take samples of heterogeneous landscapes. Near-infrared images captured from multispectral sensors help distinguish plants from soil and water due to spectral differences (Tay et al., 2018). Multispectral cameras with UAVs can significantly impact monitoring diversity in the grasslands and preserving it for future generations (Strong et al., 2017). In addition to offering ultra-high spatial resolution over relatively large areas at a reasonable cost, UAV-mounted sensors provide an excellent way to bridge the gap between field observation and traditional remote sensing methods (Manfreda et al., 2018). The type of sensor and spectral resolution can help define the region's vegetation more accurately at a local level (Furukawa et al., 2021). The vegetation maps make understanding distribution patterns easy, and UAVs have made vegetation surveys possible where field reconnaissance is challenging.

Vegetation indices were used to distinguish riparian vegetation from bare soil, crops, and grasses (Yang, 2007). Normalized Difference Vegetation Index (NDVI) acquired using a multispectral camera provides useful data about vegetation vigor and biomass, which is helpful for the identification of vegetation in images compared to RGB sensor-based spectral indices (Visible Atmospheric Resistant Index (VARI), Triangular Greenness Index (TGI)) (Fuentes-Peailillo et al., 2019). It was observed that RGB indices could identify the patterns but the division of different classes in the image was poor, which is important for mapping the species (Fuentes-Peailillo et al., 2019). Also, there are other RGB-based vegetation indices like Normalized Green Red Difference Index (NGRDI), Green Leaf Index (GLI), Visible Atmospherically Resistant Index (VARI), Red-Green-Blue Vegetation Index (RGBVI), which were used to predict dry matter yield of a grassland (Lussem et al., 2018). The efficiency of UAVs with photogrammetric techniques has been exhibited in agriculture as high-resolution data have helped evaluate various vegetation indices

(Candiago et al., 2015). The classification accuracy of the images of a landcover and vegetation types can help evaluate the area's natural regeneration process (Furukawa et al., 2021), which requires planning and monitoring of the area for future purposes.

UAV-acquired two-dimensional images are reconstructed in a three-dimensional structure, which can be processed using Structure from Motion (SfM) photogrammetry. With low-cost methods for high-resolution images, SfM helps construct 3D structures using the number of overlapping images for feature extraction, matching, and refining reconstruction using bundle adjustment (Schonberger and Frahm, 2016). SfM is also helpful in generating dense 3D point clouds with high quality and can be used to create Canopy Height Models of the forest areas but is unsuitable for dense canopy trees (Mlambo et al., 2017). Using LiDAR-derived CHMs is expensive compared to UAV SfM-derived CHMs, which are useful for ecological studies and can help in improving classification accuracy (Prošek and Šímová, 2019a).

In the environmental research community, researchers utilize various image processing techniques to extract information that helps analyze the scenario based on environmental parameters for monitoring purposes. Similarly, the Object-based Image Analysis (OBIA) method is used, which uses the image segmentation process and is more prevalent among the researchers while implementing different image processing techniques. Image segmentation implies partitioning any images based on their homogeneous characteristics, which further help categorize similar objects. The specific blocks of the segmented images help to analyze while categorizing the objects into small units based on similar context, spectral value, or spatial information. These spatial, spectral, and contextual properties of the segmented images further help the researcher monitor the changes over the decades and so on (Johnson and Ma, 2020). Object-based image analysis technique is a robust approach in vegetation studies while extracting significant features. In past studies, proven object-based image analysis is a beneficial and powerful method for working with UAVs based on high-resolution RGB(Red, Green, Blue) images (Grybas and Congalton, 2021; Yang et al., 2022; Zhou et al., 2021). The advantages of working with UAV-based images are economical, flexible, and high resolution. It offers massive information about vegetation, including precise shape, color, texture, and geometry. This information further helps to improve the homogeneity within the image pixels and influences the accuracies of the segmentation algorithm of object-based image analysis(Zhou et al., 2021). OBIA has proved to be better for vegetation mapping (Grybas and Congalton, 2021; Liang et al., 2020; Yang et al., 2022). When accurate landcover maps are limited for an area, OBIA can be a valuable method for vegetation classification, which can be used for future monitoring. For the classification of imageries, object-based classification has resulted in better vegetation maps compared to two pixel-based classifications (Kamagata et al., 2006).

Machine learning is a powerful tool for qualitative vegetation mapping, and Random Forest is one of the popular classifiers used for large datasets. A random forest is an ensemble of decision trees using a set of data to make predictions (Belgiu and Drăgu, 2016). Millard and Richardson, (2015) have mentioned the Random Forest as one of the most commonly used classification algorithms and is highly sensitive to the size of the training datasets. The same authors state that training samples are essential to improve classification accuracy, and their impact can be seen in their study.

During the process of classification of vegetation in different landscapes, vertical information plays a crucial role in differentiating the vegetation into different life forms, for which GCPs are helpful. GCP plays a critical role during georeferencing of the images as the number and location help improve UAV accuracy (Sanz-Ablanedo et al., 2018). It was evident in the results that 3D root mean square error (RMSE) improves when more GCPs are used, like an error in Z-component reduced from 20cm to 8cm when 18GCPs were used instead of 4GCPs (Gerke and Przybilla, 2016). For many years, researchers have been working with Digital Surface Models (DSM) and orthoimages, for which accuracy is essential. With the improvement in UAV photogrammetry applications, the influence of the number of GCP for georeferencing DSM is evident (Agüera-Vega et al., 2017b). Gerke and Przybilla, (2016) mentioned that bundle adjustment is influenced by the flight directions and altitudes (cross flight), as RTK-option improves the absolute image orientation and reduces block deformation. The technological advancement of UAVs is improving each day, and in the present scenario, there are several types of models of UAVs to be used. It is a practical approach of using vertical data with spectral data derived from UAVs to improve classification accuracy (Prošek and Šímová, 2019b). To generate 3D models, creating orthophotos requires the highest possible accuracy, for which good distribution and optimum number of GCPs are recommended (Awasthi et al., 2020). The horizontal and vertical accuracy was improved when GCP was used for georeferencing the products of UAV photogrammetry, such as orthophotos and DSM (Agüera-Vega et al., 2017a). So, such results promote the application of UAV photogrammetry, especially in highly risky study areas. A study also showed the significance of vertical information (derived from UAV SfM) with multispectral data of the shrubland vegetation helps in improving the accuracy of the classification and can be a cost-effective method for its mapping (Prošek and Šímová, 2019b).

Multi-temporal data of Unmanned Aerial System(UAS) have proved significant in improving the accuracy of classification of forests at the species level by using RGB and multispectral (MS) imageries (Grybas and Congalton, 2021). Similarly, the multi-temporal imagery of UAS was used for the comparison of the canopy cover model derived from RGB and MS sensors, which resulted in the MS sensor being stable and accurate, but RGB-based estimation of canopy cover can be a suitable alternative to MS (Ashapure et al., 2019). The classification accuracy of mapping the vegetation can be improved by using multi-seasonal imageries from Sentinel-2, which can narrow down the errors while classifying and be highly informative about the vegetation in the study area (Macintyre et al., 2020). For landscapes with similar vegetation, it is difficult to detect the changes in the species unless it is acquired in different seasons. This study will consider the heterogeneous landscape in mapping dominant life-form classes using high-resolution multi-temporal data.

1.2. Research problem

Mapping vegetation is essential to understanding species distribution and deriving important landscape information. UAV and field reconnaissance is invaluable (Müllerová et al., 2021). In heterogeneous landscapes, detecting changes in vegetation in the short to medium term at a fine scale can be challenging (Motzkin et al., 1999). So, a detailed and accurate vegetation map is necessary to assess the effect of the conservation practices in the area of interest. Field-based methods and satellite data have been used, which is more time-consuming and expensive. Satellite imageries cover a large area but are not helpful for detailed vegetation maps. So, this study was done to find the solution to unanswered questions. This research will help investigate the components that can improve the accuracy and precision of vegetation mapping of large heterogeneous landscapes with the combination of field methods and UAVs in different aspects. It aims to find more straightforward and cost-effective methods for classifying different vegetation types present in the area with good classification accuracy. It is necessary to improve the classification accuracy for the vegetation maps. Integrating UAV using different sensors with field surveys can help transform the tedious monitoring task into more functional and accurate maps that will take less time than traditional methods. Using the same methods and comparing the classification accuracy of vegetation maps in different conditions will help understand the best conditions and inputs required for vegetation mapping. A comparison between classification using different image formats will help in selecting parameters during the flight planning. While comparing the sensors results will help in determining the importance of spectral information in generating vegetation maps. Also, this study will help to investigate the seasonal effect in vegetation mapping and determining parameters for flight planning. UAV photogrammetric methods for vegetation mapping using GCPs will help in better georeferencing which can be helpful to align the multi-temporal UAV imageries. These combination of imageries can be used with field surveys for monitoring the changes in a period of time. It is important to select the best parameters to generate an accurate vegetation maps. So that such maps can be used to make an informative decision for its conservation and management for future reference by the end-users.

1.3. Research objectives and research questions

1.3.1. General objective:
This research aims to assess the effectiveness of UAVs with GCP in vegetation mapping to monitor the dominant life forms in a heterogeneous landscape. The research focuses on improving a vegetation map's classification accuracy based on image compression, sensor, and seasonality. The research objectives, research questions, and hypothesis are as follows.

1.3.2. Specific objectives

R.O.1: To evaluate Multispectral and RGB images for mapping vegetation at the dominant life form level.

R.Q.1.1: What is the effect of image compression (JPEG format) in image classification?

Hypothesis: Uncompressed (DNG/TIFF format) UAV imagery results in higher classification accuracy.

R.Q.1.2: Is vegetation classification accuracy with RGB-UAV data significantly different from MS-UAV vegetation classification?

Hypothesis: Vegetation classification accuracy with MS-UAV is significantly better than RGB-UAV imagery.

R.O.2: To assess the importance of GCPs to improve accuracy in vegetation mapping.

R.Q.2.1: What is the effect of GCPs on point cloud density and vegetation structure using point clouds?

Hypothesis: GCP can improve vertical information extracted from SfM processing as it decreases the potential deformations in the block.

R.O.3: To assess the usefulness of tri-seasonal UAV image classification (Winter, spring, and summer) in vegetation classification accuracy.

R.Q.3.1: How do combined UAV images from three seasons affect classification accuracy compared to a single-season image classification?

Hypothesis: The combination of winter, spring, and summer UAV imagery will result in higher vegetation classification accuracy than individual season data.

2. STUDY AREA & METHODS

2.1. Study Area

The Greater Côa Valley is an area of 312.000 hectares located in the Guarda district in Beira Interior, which borders Northern Portugal and Spain. It includes seven municipalities (Figueira de Castelo Rodrigo, Pinhel, Vila Nova de Foz Côa, Trancoso, Almeida, Mêda, and Sabugal). It has a mean population density of 22.3 ± 13.6 inhabitants/km² (INE, 2011), concentrating most population in the capital of the district, Guarda (55.5 inhabitants/km²), with much lower densities in the rest of the area (minimum densities found in Almeida, 11.7 inhabitants/km²). Côa Valley comprises the Côa river watershed from the Malcata mountain ranges in the south and contributes to the Douro River in the north. It is a part of the Iberian Peninsula, with Dehesa, Montado, and Sierra landscapes having a natural habitat state due to various ecological processes.

The dominant land covers of Côa Valley (are transitional woodland-shrub (23.48 %) and moors and heathland (16.48 %) (CLC, 2018). This is the result of the gradual abandonment of marginal agricultural regions since the rural exodus of the 1950s (Copernicus, 2018). Agricultural land is the most common form of Land use but is covered by natural vegetation under extensive use for livestock production. Vineyards, olive, and almond groves are important land uses in the lower Côa, which already benefit from the microclimate the Douro canyon provides ("Rewilding Europe," n.d.). *Figure 1* demonstrates the picture of the Greater Côa valley in Portugal. Two different sites in the valley are Vale de Madeira (also known as Ermo das Águias) with six plots and Vale Carapito with five plots.

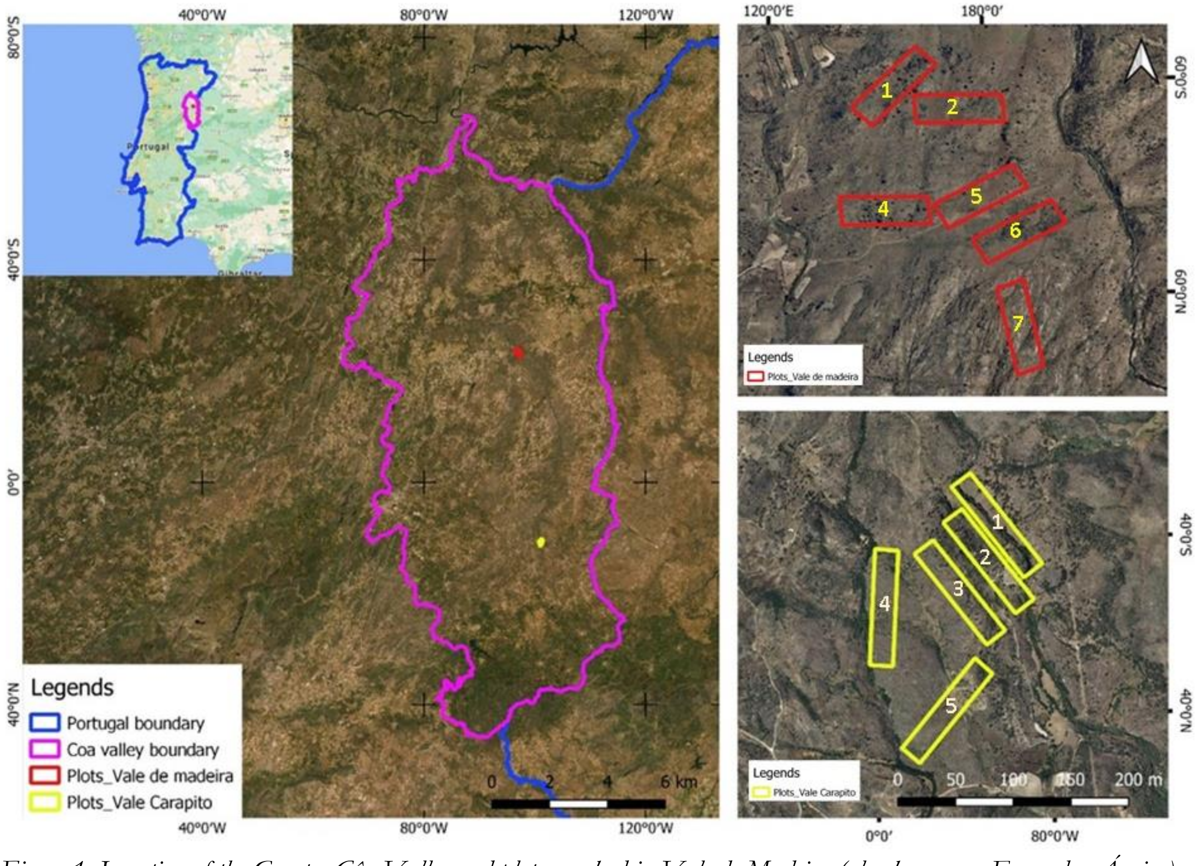

Figure 1: Location of the Greater Côa Valley and plots marked in Vale de Madeira (also known as Ermo das Águias) and Vale Carapito

The Côa valley area was abandoned, leading to a unique and novel opportunity for its conservation by rewilding the area. The browsing activity by horses and wild goats helps to manage the spread of scrubs and brooms, which leads to the maintenance of pasture areas and vegetated woodlands, preventing the risk of wildfires (DeSilvey and Bartolini, 2019). The Côa Valley is one of the wild areas of Portugal, with more than 100,000 hectares of land designated as Natura 2000 zones, with a variety of semi-natural and natural habitats ("Rewilding Europe," n.d.). In the Côa Archaeological Park, over a thousand engravings dating back 25,000 years are etched into the rocks of this valley, which is listed as a UNESCO World Heritage Site (Thomas, 2019) and also the "Faia Brava Reserve," the first private protected area in Portugal.

Climate: This region experiences a Mediterranean climate of hot, dry summers and cold winters. The Côa valley has a significant climatic condition as winter is cold and mild compared to hot summers when the temperature is above 30°C. The rainfall is evident more during winters than summers. During summer, sometimes tributaries may dry up (Zilhão et al., 1997). The landscape with natural vegetation reflects the Mediterranean ecosystems. Such ecosystems are abundant with evergreen species compared to deciduous ones, and vegetation is characterized by the presence of trees, woody shrubs, and sclerophyllous leaves (Joffre and Rambal, 2001).

Geography and species composition: The *Côa* river crosses the area from the South (the river source) to the North (the river mouth). In the Northern area, the *Côa* Valley is characterized by a typical Mediterraneanhabitat interspersed with fields of olives, almonds, and cereals. The valley has a mixture of oak forests, scattered fields, and rocky heathlands. In *Serra da Malcata*, in the South, vegetation is dominated by dense shrubs, industrial plantations of *Pinus* spp., eucalyptus, and Douglas fir (*Pseudotsuga menziesii* (Mirb.) Franco), and scattered woodlands of holm oak (*Quercusrotundifolia* Lam.) and Pyrenean oak trees. Recent socio-economic changes led to land abandonment and a continuous rural exodus, creating opportunities for landscape restoration. Cork oak (*Quercus suber*) is also present as one of the dominant species in the area.

Vale Carapito: A plot (plot number 5) in Vale Carapito was considered for objectives 1 and 2. Vale Carapito is present to be in the North of the historic village of Vila Maior, two kilometers from the east bank of the Côa River. Vale Carapito displays a diverse natural habitat & different ecological condition (like mixed coniferous and hardwood forests, scrubs, and meadows) for plants and animals, surrounded by the Alfaiates stream and Cesarão river. There have been fire incidences in the area, which last occurred in 2001 and 2002 when 15,82 hectares (26% area) were burned.

Figure 2: Sorraia horses introduced in Ermo das Águias

During the 20th century, agriculture used to be the primary occupation in the landscape, which has now turned into an abandoned area where the rewilding process is evident, as various species of oak, alders, and ash tree roots are seen. As the rewilding process has improved, the territory can be seen with the presence of Sorraia horse and fawn, which used to be in abundance. Sorraia horses are similar to wild horses, which used to be inhabitants of western Europe. However, this time, they are introduced into the valley by the Rewilding Portugal to replicate the role of its ancestors in the ecosystem, which helped to improve the nutrient cycle and positively impact amphibians, reptiles, small birds & insects, and enriching biodiversity. Considerable diversity of species is found in the valley, where Vertebrates include Pisces, amphibians, reptiles, birds, and mammals. Insects include butterflies, moths, scarabs, bees, wasps and ants, cicadas, and bed bugs. Among plants, about 21 species of trees and bushes, ten species of nationally threatened species, six species are internationally threatened, and 11 species are the Iberian endemic ("Rewilding Europe," n.d.).

Ermo das Águias: A plot in Ermo das Águias was considered to study the effects of image acquisition season on vegetation classification. Ermo das Águias is the area on the west bank of the Côa river and represents an important transition in the valley. The area has gentle slopes that are edged with rivers having rugged cliffs and leading to the mouth begin of the Douro River. The fire and grazing greatly impacted the area, leading to bushes and a bare rock-dominated landscape. About 272 fire incidences occurred every five years between 2000 to 2019, affecting about 9% of the area. The groves of black oak, cork oak, and small holm oak are present naturally in the area. The wet meadows recover floristic diversity, which is highly suppressed by the grazing and affects the area's productivity. Griffon vulture, golden eagle, and black stork are some emblematic birds found in the region as predators. It is also the first place to introduce Sorraia horses, as in *Figure 2*. As per the first survey, the area was focused on plants and insects, among which five species are nationally threatened, eight are internationally threatened, and 6 are Iberian endemic species ("Rewilding Europe," n.d.). Some exact numbers of species are in *Table 1*.

Table 1: Number of species found in Vale Carapito and Ermo das Águias

Communities	Number of species in Vale Carapito	Number of species in Ermo das Águias
Vertebrates	147	104
Insects	162	94
Plants	164	143

2.2. Methodology

The section includes the various components used for the research, a brief description of the datasets used, field data collection, image processing, and different software used for this study. The flowchart (*Figure 3*) shows four major phases; 1. UAV images acquired 2. Field Observations 3. UAV-SfM image processing 4. OBIA and data analysis. The sub-sections will explain the workflow followed for the study as shown in *Figure 3*, which includes different processes, and they are listed as follows:

1. Data and its acquisition
2. Structure from Motion (SfM) image processing
3. Vegetation Indices
4. Object-Based Image Analysis (OBIA)
5. Variable Importance
6. Comparison of results

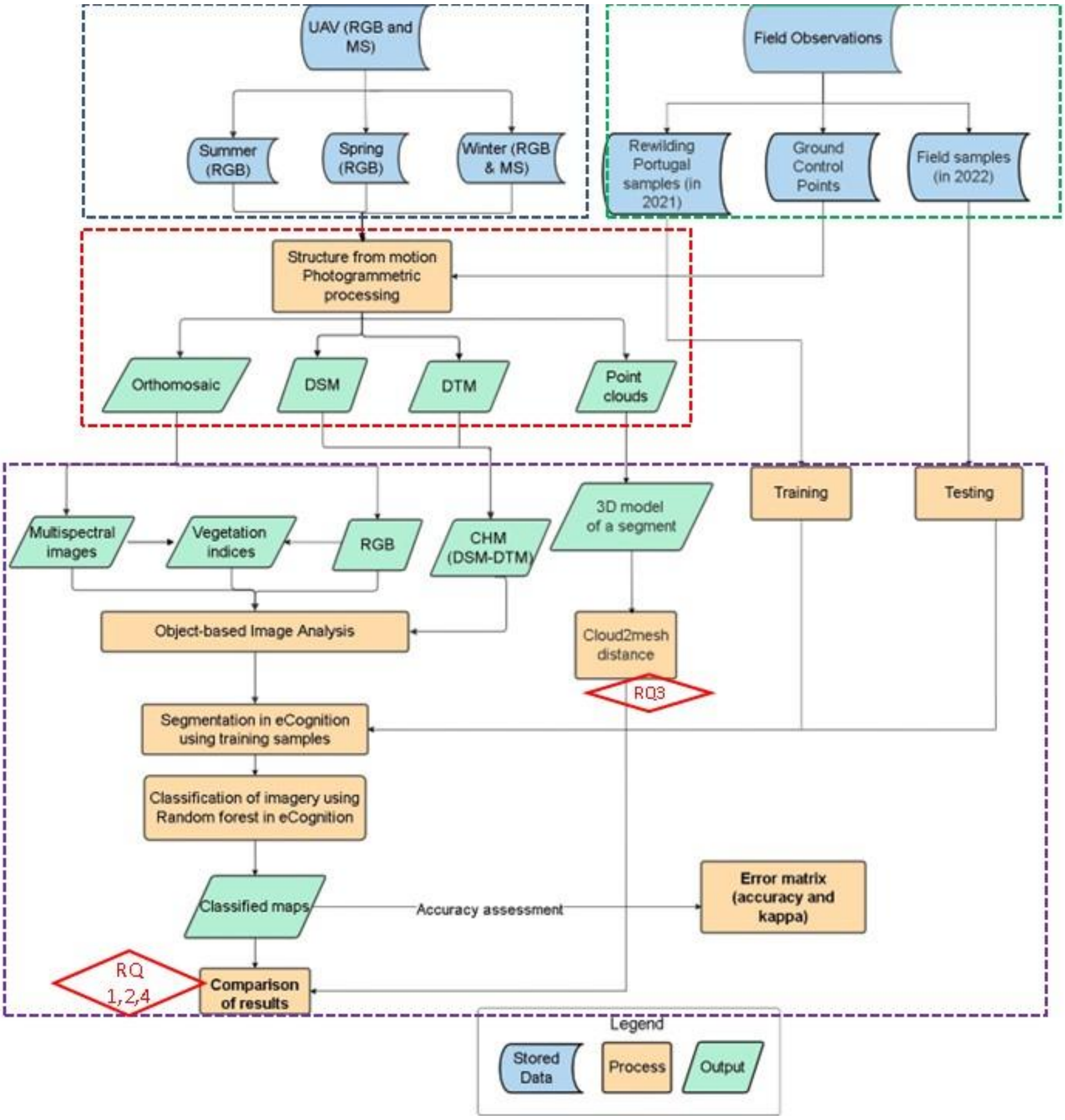

Figure 3: Overall workflow of the study

2.2.1. UAS Image acquisition

The data used for this study include UAV images acquired by Rewilding Portugal in Ermo das Águias in summer, July 2021, and in spring, May 2021, using an RGB camera (DJI Mavic Pro 2). UAV images acquired by the Rewilding Portugal were without using GCP and the flight parameters (Annex 1), which led to different ground resolution and image quality.

The UAV data for early spring (or late winter) was collected during the fieldwork in March 2022. The UAV data consisted of Multispectral and RGB images acquired between 30th March 2022 to 2nd April 2022 using Parrot Sequoia multispectral and RGB camera of DJI Phantom4, respectively. For the study, plot 5 of Ermo das Águias and plot 5 of Vale Carapito were considered.

UAV-RGB and UAV-Multispectral images were acquired with a camera-view angle of 90 degrees, also called "nadir." The study area has almost a flat terrain, so nadir images are recommended (Seifert et al., 2019). Due to covid restrictions and unavailability of rewilding Portugal team, the data collection was made possible in March 2022.

A test flight was conducted on the first day to adjust different parameters according to the study area for the initial preparation. The land was unlevelled, and weather conditions were not favorable; this delayed the drone's flying, and image acquisition was made between 13:31 to 16:47 on March 30, 2022, in Ermo das Águias for plot 5, whereas between 13:27 to 15:41 on April 1, 2022, in Vale Carapito for plot5 (*Figure 1*). The weather conditions in Ermo das Águias were cloudy and windy due to the season, with continuous changes in illumination. To overcome this issue, multiple acquisitions were performed in the same area aiming at uniform illumination conditions. The weather conditions in Vale Carapito were sunny and bright, with scattered clouds passing over the study site at high speed. To overcome this issue, image acquisition was performed with frequent breaks only when illumination was without clouds. The flights were carefully observed with the time noted, and calibration of parrot sequoia camera was done before and after each flight.

Figure 5: DJI Phantom 4 with sequoia camera and sunshine sensor in the field.

A DJI-Phantom 4 camera was used to acquire UAV-RGB images, and a Parrot Sequoia multispectral sensor was used to acquire UAV-Multispectral images. The sensor has four cameras, each with different spectral bands (Red, Green, Red-edge & Near-infrared) to capture the images. The sequoia camera also gives RGB imagery simultaneously. The Sequoia has a sunshine sensor which is useful to measure the intensity of light and compensate for the exposure as per the condition of the sun ("Parrot Sequoia," n.d.). The Sequoia camera (on the bottom) and sunshine sensor (on the top) were mounted on the quadcopter DJI Phantom 4, as shown in *Figure 5*. A parrot sequoia calibration plate (*Figure 4*) was used for radiometric calibration. The calibration was done after each flight because of the change in illumination.

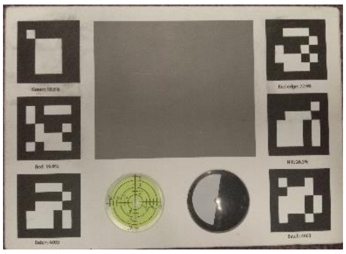

Figure 4: Calibration plate (Parrot Sequoia)

2.2.1.1. Flight planning

Flight planning plays an essential role in acquiring the UAV images of a study area. The flight planning for this study was done using UgCS for DJI, which can be operated using a laptop or android phone and is compatible with both modes of use. UgCS application was used to create the flight plans (or missions) for the acquisition of the images of the study area ("UgCS," n.d.). The advantage of UgCS was to decide the Ground resolution on a prior basis as the UAV maintains a particular flying height throughout the flight. The flight parameters are mentioned in *Table 2*, and the flight plans are in Annex 2.

Table 2: Flight parameters used for the UAV image acquisition in the study areas

Flight Parameters	**Vale Carapito**	**Ermo das Águias**
Flight speed	4.50m/s	5.00m/s
Ground resolution	2.50cm	2.50cm
Forward overlap	80%	80%
Side overlap	85%	85%

The drone was connected to an android phone (using the UgCS android application), which was connected to the controller. The sequoia camera was connected to different mobile, and the parrot sequoia application was used to start and stop the camera. It was also used to capture the images of the calibration plate, which is used to calibrate while processing the captured images. A high percentage of front and side overlap was used in order to improve accuracy by creating more match points in the images during processing. Also, the weather conditions were not ideal for the data acquisition.

2.2.1.2. RGB images

The team of Rewilding Portugal acquired RGB images for Ermo das Águias using the RGB camera of Mavic Pro 2. The flight resulted in a total of 1082 images (for July 2021) and 870 images (for May 2021) covering the area marked by the team. The raw UAV images were in DNG format, which was changed to TIF format for processing using the Structure from Motion approach in Pix4D. Plot 5 in Ermo das Águias was considered as the study area to assess the seasonality effect on the vegetation classification accuracy. In contrast, Vale Carapito (plot 5) will be considered the study for comparing image formats, the significance of GCP, and the comparison of the sensor.

In March 2022, plot 5 of Ermo das Águias and plot 5 of Vale Carapito were considered for the study. The DJI Phantom 4 camera was used for the RGB images (as it gives better image quality than Parrot Sequoia). The images were collected in the form of raw DNG format and JPEG format. A total of 988 images have resulted for plot 5 of Vale Carapito. Whereas for Ermo das Águias 796 images. Multiple flights for the same area resulted in a high number of images. The images will be selected during the image processing to generate orthomosaic.

2.2.1.3. Multispectral images

Parrot Sequoia sensor was mounted on the drone for multispectral imagery. The data acquisition using MS sensor was made only in March 2022. The sensor has four cameras (Red, Green, red-edge, NIR), each lens resulting in one image and one RGB image (a total of 5images each time). For Vale Carapito, a total of 1744 images have resulted for plot 5, and for Ermo das Águias, 2564 images. Also, a few images of the calibration plate which will be used for radiometric calibration during SfM processing in Pix4D. The images will be selected during SfM image processing in Pix4D.

2.2.2. Ground Control Points (GCPs)

Ground Control Points (GCPs) are effective for georeferencing and help reduce errors during UAV photogrammetric processing of images (Martínez-Carricondo et al., 2018). GCP was not marked in 2021 and was collected during

Figure 6: Target mark used as GCP in the study area

fieldwork for data collection in March 2022. As the number of GCP and their distribution influence accuracy (Awasthi et al., 2020), GCPs were distributed before the flight, and measurements were taken using the Global Navigation Satellite System (GNSS) after the flight and re-collected the target marks from the area. The target marks were positioned on the ground using wooden pegs, as shown in Figure 6. Around 13 to 15 targets were placed on the ground and well-distributed throughout the area. Since the ground was unlevelled, targets were placed on each corner and center of the plot, aiming to observe the ground level change while measuring altitude (Z value) using differential GNSS. All the ground data measurements were recorded using GNSS LEICA GS15 by configuring the device for the Portuguese network service to use Real-time Kinematic (RTK) correction. Differential RTK corrections are gathered at a base station (it usually reports the base station location used) and transmitted to the rover, which is correcting the signal from the satellite in real-time, achieving positional accuracy of <5cm. GCPs were stored in WGS84 geographic coordinate system. During the field data collection, mobile SW maps and google earth applications were used to mark the targets placed in the actual plot size and to know the boundary of the study area.

2.2.3. Field Observations

The field observations are essential as they are used for training and validation purposes of the study. For the study, land cover and vegetation typology was identified and selected based on the discussion with the Rewilding Portugal team. The observations in Ermo das Águias were collected by Rewilding Portugal in May and July 2021, whereas in Vale Carapito in May and July 2020. These are used as training samples for the classification. Around 187 samples for Vale Carapito and 369 samples(of two seasons) for Ermo das Águias were used as a training dataset for seven classes.

In March 2022, SW maps were used for the field data collection, all the necessary information was recorded, and photographs were taken for reference. The points recorded were used as a validation dataset. About 105 points were collected in March 2022 for seven classes at each site. These validation samples are independent of the training samples. The samples are polygons created in ArcMap 10.8, then saved as a shapefile. A few additional points were collected for the Ermo das Águias to differentiate between deciduous and evergreen trees. Since Ermo das Águias was recorded by the Rewilding Portugal team during spring 2021 and summer 2021, the observations during March 2022 helped analyze the same areas for three seasons, and the samples were recorded to be used for vegetation classification accuracy of multiple seasons. Some photographs were taken of the references. In addition, lichens were the additional class observed in the Vale Carapito site as they were found in dominant form throughout plot 5. The samples were collected during the field visit and were found in dried form. The species were identified based on the main plant life-forms used by Kuchler's method of description(1967); the criteria used were plant size (height) and plant function (deciduous or evergreen) (Kent, 2012). The classes considered for the classification will be helpful in future monitoring purposes.

Land cover and vegetation typology

The study area was a heterogenous landscape with the presence of horses in the Ermo das Águias plot, while in Vale Carapito, there was evidence of grazing animals too. The vegetation typology varied in the different sites. The presence of rocks and bare soil was found in a significant part of the study area, so the land cover classification was considered for this study. The classes considered for vegetation classification

Figure 7: Deciduous oak trees and dried lichens (in picture1), Evergreen oak trees in an exclusion plot (picture2), and dominant white broom shrub (picture3) in the study area (Vale Carapito).

Figure 8: Evergreen oak tree surrounded by dominant white broom shrub (picture1), the dried form of bracken during winters (picture2), shrubs and rocks major land cover in the plot of Ermo das Águias (plot5)

were: trees (deciduous or perennial), shrubs, grass, bare soil, bracken, lichens, and rock. The major form of vegetation found can be seen in *Figure 7* and *Figure 8*, showing the Vale Carapito and Ermo das Águias. Trees found in the area were species of pines and oaks, among which some oaks were deciduous (*Figure 7)* in Vale Carapito and some evergreen(*Figure 8*) in Ermo das Águias. The lichens were found in dried conditions (as shown in *Figure 7*) because the area suffered from high temperature and low water conditions. The dominant shrub in the study area was the white Spanish broom (*Cytisus multiflorus*), as shown in *Figure 7Figure 8*. The shrub was flowering in the early spring season and was dominated in the area.

2.3. Structure from Motion Image Processing

It generally includes data processing for which UAV-RGB and UAV-MS images were processed. The photogrammetric processing of UAV images is the primary step for data processing. It includes the generation of orthomosaic, Digital Surface Model (DSM), Digital Terrain Model (DTM), and point clouds.

2.3.1. Pre-processing

Before photogrammetric processing, it is essential to check that the images acquired are of good quality. It is necessary to remove all the blurry, unrequired, repeated, wrongly captured, or oblique photos before SfM processing. The alignment of the pictures, resolution, coordinate system, and extent were checked using

ArcMap 10.8.2 software. During pre-processing, raw images (DNG) are converted to multiband TIF images using Adobe Photoshop 2020 software. The RGB image's resolution is 300dpi*300dpi (horizontal and vertical resolution), as these are uncompressed images. The images were processed in batches and will be used for creating orthomosaics and point clouds. On the other hand, RGB-JPEG images have a resolution of 72dpi*72dpi (horizontal and vertical resolution). In comparison, MS images were in TIF format and had a resolution of 96dpi*96dpi (horizontal and vertical resolution).

2.3.2. UAV Data Processing

Structure from motion is applied for the data processing of UAV-RGB and UAV-MS images. The photogrammetric processing was done using Pix4D Mapper software. The SfM processing of UAV images is done with the Ground Control Points recorded during the field visit. The GCPs are recorded using GNSS LEICA GS15 (Portugal's number for RTK correction). While creating projects with GCPs, a total of 10 GCP and four checkpoints were used in each case. The distribution of images and GCP in map view (Pix4D) is added in Annex 3. The results of SfM processing in Pix4D are given in Annex 4.

2.3.3. Orthomosaic generation

The SfM processing produces orthomosaic, point clouds, DSM, and DTM and involves three process steps ("Processing steps - Support," 2022). JPEG and TIFF images were separately processed using the '3D maps' template for RGB images, while for Multispectral images 'AG Multispectral' template was used for processing. In the first step, key points in the images are extracted and matched; also, the camera parameters are optimized. In the initial processing, a full image scale was used for the study; for matching image pairs 'Aerial grid' was selected, and for calibration, targeted number of keypoints was 'automatic', calibration method was 'standard' and camera optimization for internal and external as 'All'. The processing will use overlapping images to identify the matching key points between the 2D images and, as a result, create sparse point clouds (Mlambo et al., 2017; Schwind and Starek, 2017). Before proceeding to the second step, GCP was imported, and the 3D position of GCP was marked on the images for georeferencing of the project. The GCP was used while creating the project and was marked on images to generate orthomosaic, as this will help overlap the layers perfectly. The 3D point clouds were generated using bundle block adjustment. The end step was to generate orthomosaic and DSM. DSM was generated using inverse distance weighting, while DTM was generated using point cloud classification, in which five different point groups are used to classify the point clouds, parameters details are shown in *Table 3*. The classes are Road surface, buildings, ground, high vegetation, and human-made objects ("How to generate point cloud classification," 2022). The index calculator was not used to generate the vegetation index because of an unresponsive error of the software. So, eCognition was used to generate vegetation indices.

Table 3: Parameters used for Pix4D processing of RGB images

Point Cloud and Mesh (Point Cloud)	Image Scale: Original Point density: Optimal Max number of matches: 3 Classify point clouds
Point Cloud and Mesh (3D Textured Mesh)	Generate 3D textured mesh Settings: High resolution
Point Cloud and Mesh (Advance)	Default settings
DSM, Orthomosaic and Index (DSM and Orthomosaic)	Resolution: Automatic DSM filters: Use noise filter and surface smoothing (Sharp) Raster DSM: Inverse distance weighting Orthomosaic: GeoTIFF

DSM, Orthomosaic and Index (Additional outputs)	Grid DSM: LAS Raster DTM: GeoTIFF DTM resolution: Automatic (5*GSD)
DSM, Orthomosaic and Index (Index calculator)	Radiometric (for RGB): No correction Resolution: Automatic Downsampling method: Gaussian Average

Multispectral images were processed with almost similar settings as in table 3 but with some changes. In Initial processing, calibration method was alternative. Point density was selected low in point cloud and mesh, while radiometric calibration was used in the index calculator.

Orthomosaic created using JPEG and TIFF image format acquired in summer and spring were not overlapping each other. This shift was corrected using georeferencing tool manually to use the orthomosaic for the study. A similar case can happen in orthomosaics generated with GCP and without GCP. The presence of GCP will accurately position the orthomosaic compared to without GCP orthomosaic. So, a shift in the orthomosaic may happen. The parameters used for image acquisition by Rewilding Portugal and details are added in Annex 1. To understand and answer research question 4, Ermo das Águias was used as the study area where three seasons, spring, summer, and winter, were processed using manual tie points to overlap the orthomosaic perfectly. Each season's ground resolution was different due to different flight parameters, so each orthomosaic was resampled to 2.5cm.

2.3.4. UAV point clouds

UAV-RGB imagery generated the 3-D point clouds using Pix4D mapper software. Two sets of point clouds were generated; one was georeferenced with GCP acquired during a field visit, while another point cloud was generated without GCP but was georeferenced using the estimated camera positions. The Canopy Height Model (CHM) of 3D point clouds of two different conditions was compared using *.las dataset format. CHM is generated by subtracting the Digital Terrain Model (which represents elevation of the ground) from Digital Surface Model (which shows the elevation of vegetation) (Matese et al., 2016), as

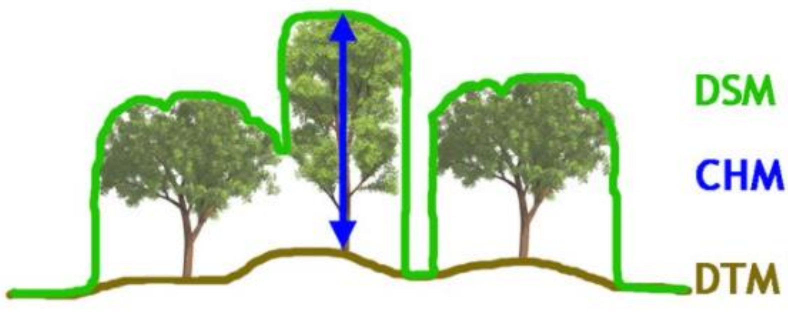

Figure 9: A pictorial depiction of creating the Canopy Height Model (Perko et al., 2011)

shown in *Figure 9*. DTM and CHM were extracted from point clouds using cloudcompare. CHM results using cloudcompare will help to understand the importance of GCP in classifying vegetation.

Cloud compare software was used for the analysis of the point clouds generated. The point clouds generated were of the same plot, but the only difference during SfM processing was with and without GCP. We have registered point cloud A (georeferenced) and point cloud B (non-georeferenced). The point cloud B was in the local coordinate system, whereas point cloud A was georeferenced earlier with Ground Control Points (GCPs).

The point clouds of both datasets were loaded in CloudCompare to understand the distance between "cloud to cloud," where the point cloud generated using GCP was used as 'reference,' and another point cloud was 'compared'. Since point clouds were not appropriately registered, the Iterative Closest Point (ICP) algorithm was considered to be used for better registration of point clouds. ICP algorithm searches for pairs of nearest points in two adjacent scans and further calculates the transformation parameters between the two clouds (Rajendra et al., 2014). The root mean square error (RMSE) for fine ICP registration for two-point clouds A and B was observed at approximately 1 m.

ICP resulted in better registration of clouds, but the RMSE was high. Due to the high computational power required, a segment was created to generate the CHM to compare the two point clouds. Using the Cloth Simulation filtering (CSF) algorithm to determine the ground points in the point clouds resulted in mesh (D'Urso et al., 2018), where the mesh is the simulation of ground. The cloth resolution was 2.0; max

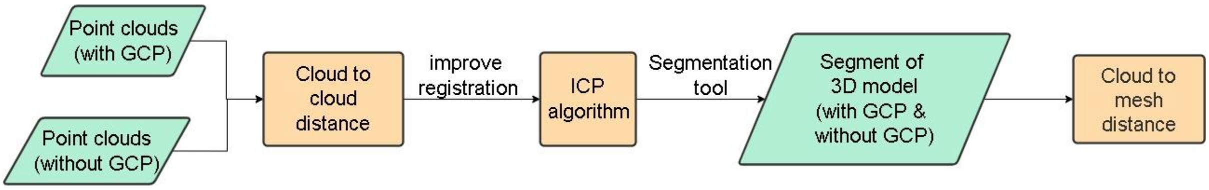

Figure 10: Flowchart of generating segment of generating CHM from point clouds

iterations were 500, and the classification threshold was 0.5. Cloth resolution refers to grid size, maximum iterations refer to terrain simulations, and classification threshold refers to classifying point clouds into the ground and non-ground. The 'cloud to mesh' parameter was used to understand the importance of GCP in generating the Canopy Height Model (CHM) and estimating the vegetation structure's vertical information. The point cloud of the whole plot was not used for the analysis, so a segment was generated using a segmentation tool. The segments of the same region were created from the point clouds (with GCP & without GCP) in which trees, shrubs, and grasses are visible. The results were generated using the 'cloud to mesh' distance tool. The results gave a Canopy Height Model of each segment, which was used to compare results ("Cloudcompare forum," n.d.). *Figure 10* depicts the flowchart to generate CHM using point clouds.

2.4. Vegetation Indices

Vegetation indices were calculated for better segmentation and classification. Vegetation indices were decided based on the literature and were different for RGB images and Multispectral images classification. These were calculated using the "layer arithmetics" algorithm, where formulas were inserted for the calculation in eCognition software. The indices used are in *Table 4* & *Table 5*, with the reference in Annex 5. The indices layer was added with 3 RGB and Canopy Height Model (CHM) layers in eCognition for RGB image vegetation classification. For MS image vegetation classification, four image layers, CHM and indices layer, were used.

Table 4: Vegetation indices used for RGB imagery in eCognition

Spectral Vegetation Indices (RGB)	Equation
GLI (Green Leaf Index)	$(G^2-R-B)/(G^2+R+B)$
NGBDI (Normalized Green Blue Difference Index)	$(G-B)/(G+B)$
RGBVI (Red Green Blue Vegetation Index)	$(G^2-R*B)/(G^2+R*B)$
MGVRI (Modified Green Red Vegetation Index)	$(G^2-R^2)/(G^2+R^2)$

NDSI (Normalized Difference Soil Index)	(R-G)/(R+G)
GRVI (Green-Red Vegetation Index)	(G-R)/(G+R)

Table 5: Vegetation indices used for Multispectral imagery in eCognition

Spectral Vegetation Indices	**Equation**
GCI (Green chlorophyll Index)	((NIR/G)-1)
NDVI (Normalized Difference Vegetation Index)	(NIR-R)/(NIR+R)
NDRE (Normalized Difference Red Edge Index)	(NIR - RE)/ (NIR + RE)
MGVRI (Modified Green Red Vegetation Index)	$(G^2-R^2)/(G^2+R^2)$
SAVI (Soil-Adjusted Vegetation Index)	((NIR-R)/(NIR+R+L)) * (1+L)
GRVI (Green-Red Vegetation Index)	(G-R)/(G+R)
NDWI (Normalized Difference Water Index)	(G-NIR)/(G+NIR)

2.5. Object-Based Image Analysis

The methodology used for this research mainly focuses on the OBIA (Object-based Image Analysis), which has proven significant in various studies (Liu et al., 2020; Makinde et al., 2016; Yang et al., 2022). Orthomosaics generated are used for Object-Based Image Analysis (OBIA), which has shown better classification results for the vegetation (Prošek and Šímová, 2019b; Yang et al., 2022). As per various studies, Object-based Image Analysis has given better results than pixel-based classification for very high-resolution imagery (Kamagata et al., 2006; Jing Liu et al., 2015; Makinde et al., 2016). OBIA helps delineate the objects, a group of relatively homogeneous pixels. It considers different properties before creating objects which are spectral, shape, texture, and spatial. (Johnson and Ma, 2020; Ventura et al., 2018). It involves two steps: image segmentation, in which an image is delineated into objects representing different features, and image classification, in which objects or segments are classified using their spatial, spectral, size, and shape properties (Johnson and Ma, 2020). Software eCognition was used for OBIA.

2.5.1. Image segmentation

Image segmentation is an essential task during the classification of various land covers, and it is crucial to delineate objects precisely and accurately. Under-segments and over-segments of the objects may lead to misclassification of the different vegetation, reducing the classification accuracy. The delineation of the different vegetation for high-resolution imagery was processed using the multi-resolution segmentation (MRS) algorithm. The segments created by MRS algorithm are based on parameters: weight of the shape, compactness, smoothness, scale parameters, & image layers used. MRS is an iterative process in which it forms an object until it acquires a threshold value for the object. The main parameter for creating segments is the scale parameter, which signifies the amount of spectral variation within objects. For the shape parameter, the higher the value, the more it is considered, and the lower the influence of color in the segmentation process. In compactness, the higher the value, the more compact the image objects will be. The pixels are merged with neighboring pixels, which are homogenous and create objects (Y. Chen et al., 2021) and are considered a bottom-up approach to aggregate pixels into homogeneous zones (Munyati, 2018). Segmentation is sensitive to the parameters used (homogeneity criteria) and image layers like CHM and vegetation indices. A trial-and-error process was used to determine the value of parameters, and a fine segmentation resulted for Vale Carapito (RGB orthomosaic, March 2022) by using; Scale parameter (SP) as 80, shape as 0.1, and compactness as 0.8, whereas for Ermo das Águias (RGB orthomosaic, March 2022) only scale parameter was changed which was 100. It was crucial to eliminate the shadows, so separate segments were considered visually, and a new class was added to remove shadows from the final classification. Another new class was artificial objects, under which target marks were segmented. Shadows and target marks were removed by the end of the final classification.

2.5.2. Classification

After segments are formed, classification is done using training samples, which are saved as a vector file. The training samples used are polygons of the different land covers and vegetation typology to be used for training the classifier model. A supervised approach is used for classification using the "Random trees" algorithm and "sample statistics based" for the source of feature space (Statistics and Assessment, n.d.). Before supervised classification, the thematic layer was used to classify sample objects into different land cover classes: Bare soil, bracken, grass, rock, shrubs, trees, and lichens. A separate class for shadows and target marks was added to carefully remove those segments in classification as it can lead to erroneous results. Similar methods were used for RGB and MS orthophoto classification.

2.5.3. Accuracy assessment

Samples collected during March 2022 field collection were used for validation and are independent of the training samples. The samples are in polygon form and used as a thematic layer in eCognition software. After classification, an error matrix of the main seven landcover classes was generated in eCognition using accuracy assessment. It resulted in overall accuracy, producer's & user's accuracy, and kappa value for the main land cover classes. Overall accuracy is generally expressed as a percentage, with 100% accuracy meaning all reference sites were correctly classified. Overall accuracy can be calculated by the number of correctly classified classes to the total number of reference classes. At the same time, the kappa coefficient helps in evaluating the classification accuracy results and ranges between the value -1 to 1, where -1 indicates poor results while +1 indicates the significance of the classification accuracy ("Accuracy metrics," n.d.).

2.6. Variable importance

Rstudio was used to determine the variable importance by generating a ggplot. It was important to assess which variable has shown more significance (usefulness) in the vegetation classification and not for selecting variables. The ggplot resulted in two metrics: Mean Decrease Accuracy and Mean Decrease Gini. 'Mean Decrease Accuracy' plots illustrate how much accuracy is lost when a variable is removed from the model, as variables are represented in descending importance. The variable is more crucial for a good classification; the more the accuracy gets affected. Whereas 'Mean Decrease Gini' is a measurement of the contribution of each variable to the homogeneity of the nodes and leaves in the final random forest model. It is based on Gini purity index. The higher the value, the higher the variable's importance in the model (Martinez-Taboada and Redondo, 2020). Variable importance plots were generated to understand which image layer plays a more important role in classification using Random Forests. The graph demonstrates the importance of each layer in decreasing order for classification accuracy. In variables, standard means 'Standard deviation' of that image layer.

2.7. Comparison of results

All the results of the classification generated are compared to answer the research questions, and the comparison is made using the classified maps and the error matrix. The error matrix generated for each result was used for the comparison. The methodology used for the vegetation classification in each case was the same: to compare the results generated using the same methods and algorithm but for different datasets. The comparison shows the effectiveness of the methodology adopted for the vegetation classification using the UAV dataset.

UAV point clouds

Point clouds were compared using the cloudcompare by generating Canopy Height Model to compare the effect of georeferencing using GCP acquired using GNSS and without GCP. The height of the different vegetation and its classification can help understand the comparison in two conditions. The comparison is made to understand if there will be an effect on point cloud density and if it will affect the vegetation classification results.

Classification results

The comparison of vegetation classification results for each question will be visually compared in which the same area will be zoomed in and compared with reference images and orthomosaic. While the main comparison will be considered using an error matrix. The same training and validation samples were used for vegetation classification to compare image format and sensors(RGB camera and Multispectral camera), as Vale Carapito (plot5) was the study area. Comparing one season with the combination of three seasons has used the same methods but different training and validation samples. This comparison was done in Ermo das Águias (plot5) as the data collection by Rewilding Portugal was in 2021, and the area did not change much in between the time. So, combining the orthophotos using multi-tie points was feasible and was used for vegetation classification.

Error matrix

Error matrix was generated in eCognition software as "Accuracy assessment," in which training and validation inputs are used. Two main metrics are considered for the accuracy assessment: overall accuracy and kappa value. Overall accuracy represents the number of correctly classified classes to the total number of reference classes. Overall accuracy can also be written in the form of a percentage. Kappa value helps evaluate the classification accuracy, i.e. more the value, the better the classification. The value ranges from -1 to +1.

2.8. Software used

A list of software has been used for the study, and they were mainly used for data processing, data analysis & interpretation, visualization, and documentation of the work. *Table 6* represents the name and the purpose.

Table 6: List of software used and its purpose

Software	**Purpose**
Adobe Photoshop 2020	Convert files: DNG (RAW) to TIFF
ArcMap 10.8.2	Pre-processing, visualization, creating maps
CloudCompare 2.12. beta	Point clouds processing and analysis
eCognition Developer 10.2	Object-based Image Analysis (segmentation & Random Forest Classification)
Google Earth Pro 7.3	Pre-flight planning, site inspection during fieldwork
Mendeley Desktop 1.19.8	Citation and referencing
Microsoft Excel	GCP recorded and data entry
Pix4D mapper 4.7.5	UAV Image processing

Parrot Sequoia 1.7.1	Camera settings & Radiometric calibration
QGIS 3.24.0	Visualization
RStudio 1.4.1106	Variable Importance
SW maps	Field survey and marking points
UgCS application	Flight planning

3. RESULTS

3.1. Structure from Motion processing

SfM photogrammetric processing of UAV-RGB and UAV-MS images in Pix4D results in orthomosaic, DTM, DSM, and point clouds. The orthomosaic of Vale Carapito plot 5 (March 2022) generated using RGB and MS images are shown in *Figure 11*. A total of 682 UAV-RGB images were used for SfM processing, 99% of which were calibrated. Different projects were created for RGB images: JPEG and TIFF with GCP and JPG without GCP. Each of the project's results was used to analyze research questions.

RGB-JPEG and RGB-TIFF were used for the classification and comparison between image formats. RGB-TIFF and Multispectral were used for classification and comparing the result between sensors. The average Ground Sampling Distance (GSD) of RGB-TIFF images was 0.0228m (2.28cm) for an area of 11.95ha. Orthomosaics show a perfect overlap, with five or more images for every pixel in most areas. The other processing results for JPEG and TIFF images are added in Annex 5. Similarly, the average Ground Sampling Distance (GSD) for Multispectral imagery was 0.0554m (5.54cm) for an area of 10.76ha. The

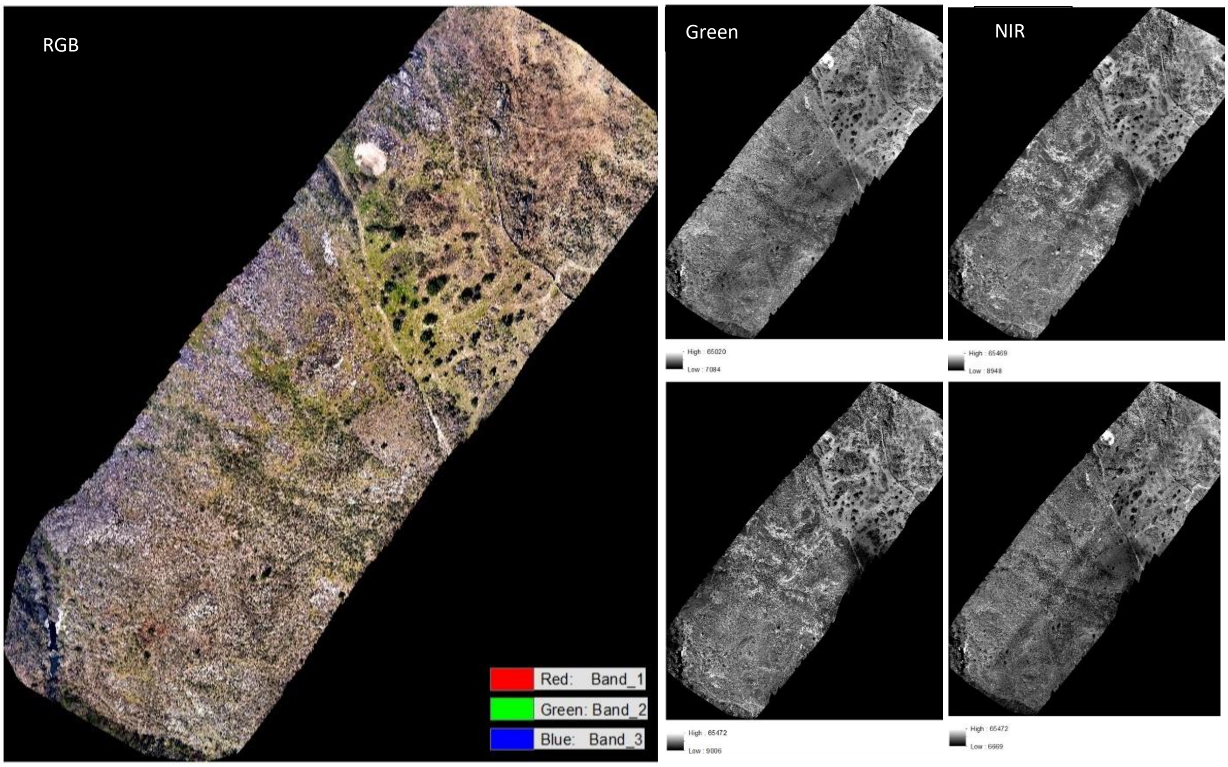

Figure 11: RGB and Multispectral orthomosaic(Green, NIR, Red-edge, Red) for March 2022 in Vale Carapito (plot5)

processing result for Pix4D is added in Annex 4.

The orthomosaic generated using UAV-RGB JPEG images with and without GCP has resulted in the same average Ground Sampling Distance, i.e., 0.028m (2.28cm). Point clouds generated using SfM processing for March 2022 using UAV-RGB images in JPEG format have resulted in an average density of 1204.68 per m^3. In comparison, the average density of point clouds for the same images but with GCP resulted 1143.45 per m^3.

Georeferencing the projects was done using 10 GCP as" 3D GCP," and four GCP was used as "check point." The mean Root Mean Square Error (RMSE) for JPEG images was 0.042m, and RMSE(X, Y, Z) were 0.04m, 0.03m, and 0.05m. The RMSE is fine as the value is almost twice of GSD value. While, for TIFF images mean RMSE was 0.029m, and RMSE(X, Y, Z) were 0.03m, 0.02m, and 0.03m. The value is comparatively better than the RMSE for JPEG images. Similarly, GCP was used during the processing of Multispectral imageries, for which RMSE was 0.054m. During processing, 10 GCP and four checkpoints were used for Multispectral imageries, and the mean RMSE was 0.054m, and RMSE(X, Y, Z) were 0.012m, 0.02m, and 0.14m. The RMSE for the height value resulted high, which signifies a high difference between initial and computed positions of GCP ("Pix4D community," 2022). It was difficult to mark GCP in multispectral images due to coarse resolution and greyscale images, so there can be chances of error. A summary of all the processing results is shown in *Table 7* for plot 5 of Vale Carapito.

Table 7: Summary of Structure from Motion results for Vale Carapito plot5

Features	UAV-RGB (JPEG)			UAV-RGB (JPEG & without GCP)	UAV-RGB(TIFF)			UAV-MS		
Number of images	682 (99% calibrated)			682 (99%calibrated)	682 (99% calibrated)			1388 (100% calibrated)		
Number of GCP	10			0	10			10		
Mean Reprojection Error (pixel)	0.145			0.145	0.135			0.231		
GCP mean RMSE (m)	0.042m				0.029m			0054m		
RMSE (X, Y, Z)	0.04	0.03	0.05		0.034	0.024	0.029	0.012	0.019	0.1
Checkpoint RMSE (m) (X, Y, Z)	0.06	0.038	0.1		0.049	0.038	0.08			
Coordinate system	WGS 84/UTM zone 29N			WGS 84/UTM zone 29N	WGS 84/UTM zone 29N			WGS 84/UTM zone 29N		
Point Cloud average density (per m^3)	1143.45			1204.68	1069.07			21.57		

Ermo das Águias

The orthomosaic of March 2022 (*Figure 12*) was generated in Pix4D, and a total of 677 UAV-RGB images (TIFF) were used for the SfM processing. The processing resulted in an average Ground Sampling Distance of 0.0225m (2.25cm) for an area of 13.14ha. A perfect overlap figure of orthomosaic is generated in which most of the pixels have an overlap of more than five images (Annex 5).

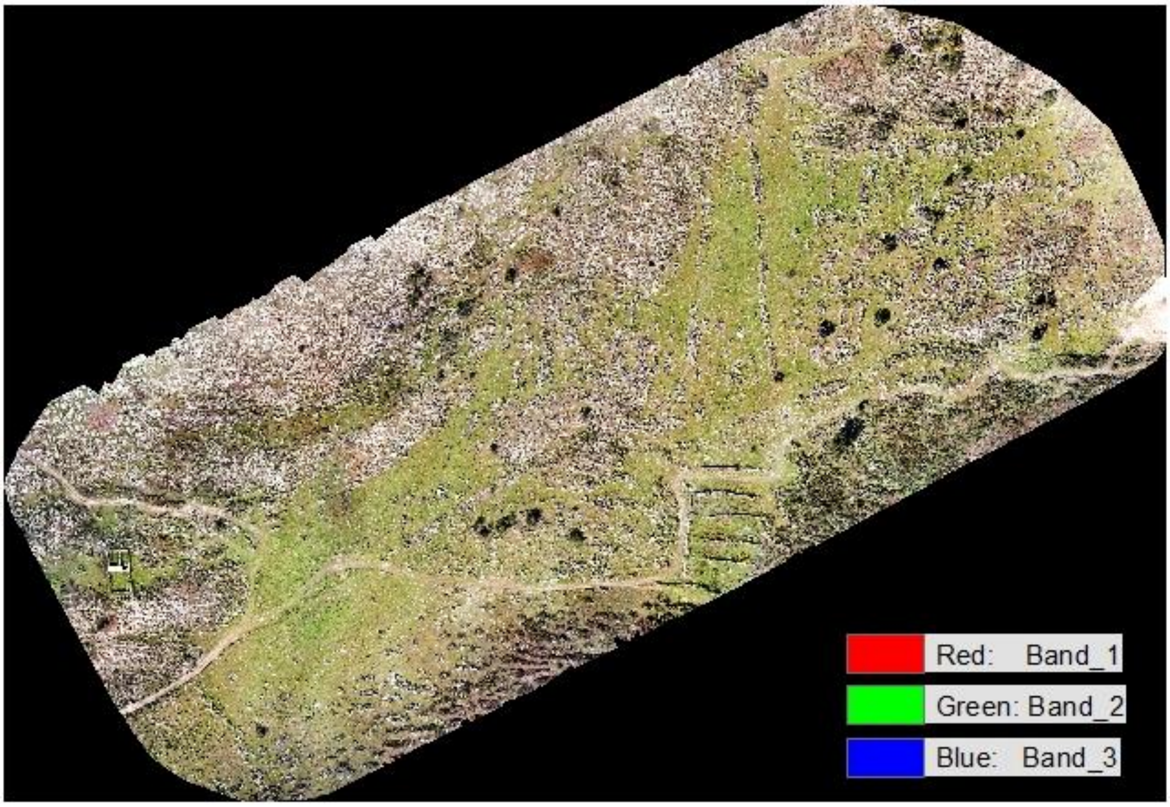

Figure 12: RGB orthomosaic of Ermo das Águias in winter season with the three different color bands

Georeferencing was done using 9 GCP as "3D GCP" and four GCP as "Check point." Average Mean Square Error was 0.043m while for RMSE (X, Y, Z) were 0.04m, 0.02m, 0.06m. The average point cloud density generated was 1135.83 per m^3. The RMSE value was fine, and the results are used for the fourth research question.

3.2. Classification of compressed and uncompressed Images format

The UAV images acquired for the research were in two formats: compressed (JPEG) and uncompressed (DNG). The vegetation classification was done with two sets of samples. At first, 119 training samples were used, which resulted in poor classification accuracy for JPEG and TIFF images. The JPEG images resulted in 59.65% overall accuracy and 0.52 kappa value. TIFF images resulted in 48.82% overall accuracy and 0.38 kappa value. The table of error matrix is shown in Annex 6. The overall accuracy and kappa value were lower in the TIFF images than in JPEG images. About 68 more samples were added to train the model, resulting in improved landcover classification. A map shown in *Figure 13* represents the vegetation classification of Vale Carapito plot 5 using JPEG images (using 187 training points).

Analyzing the classification results of JPEG images orthomosaic, it can be observed that the classifier overestimated lichens at the center of the plot, and bracken has been misclassified comparatively among all classes. Trees have been best classified among all the classes, and bracken has the lowest accuracy. Some large rocks in the plot were covered with lichens, which led to the wrong classification.

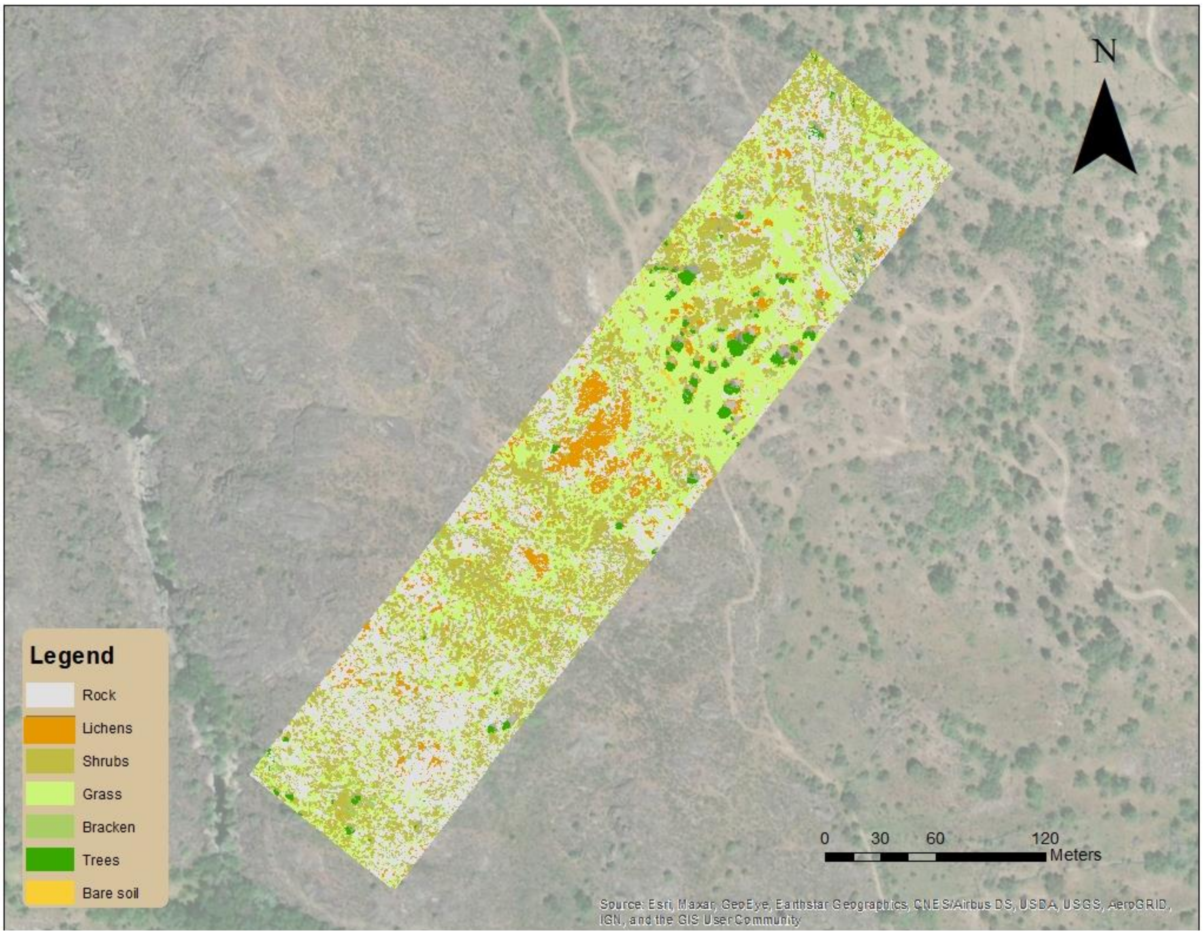

Figure 13: Map of Vale Carapito plot 5 representing the vegetation classification of JPEG images

As shown in Table 8, the error matrix improves overall accuracy using 187 training points but not with much significant change as seen in TIFF image orthomosaic. The overall accuracy is 62.04%, and the kappa value 0.54. Trees and lichens have the highest producer accuracy, while bare soil and trees have the highest user accuracy.

Table 8: Accuracy assessment of the JPEG image classification result by generating error matrix in eCognition software.

Confusion Matrix (JPEG)								
User class	**Grass**	**Bracken**	**Shrubs**	**Rock**	**Trees**	**Bare soil**	**Lichens**	**Sum**
Grass	26	1	3	6	4	4	1	45
Bracken	1	2	1	0	0	0	0	4
Shrubs	7	6	41	10	5	0	2	71
Rock	5	4	8	37	2	5	5	66
Trees	1	1	5	0	26	0	0	33
Bare soil	0	0	2	3	0	17	0	22
Lichens	7	0	0	7	0	0	23	37
Sum	47	14	60	63	37	26	31	
Accuracy								
Producer	0.56	0.18	0.69	0.59	0.70	0.65	0.74	
User	0.57	0.25	0.57	0.56	0.78	0.77	0.62	
Overall Accuracy: 62.04% **Kappa: 0.54**								

Using 187 training samples, TIFF images orthomosaic resulted in better classification than JPEG images. As the classification of other classes improved, but bracken gave the lowest accuracy among all classes.

TIFF format helps distinguish between the heterogeneous vegetation present in the landscape as it retains more information per pixel than compressed JPEG images and has high image quality (Alfio et al., 2020).

Since the area's visual image classification, as shown in ***Figure 14*** was better than JPEG image classification. So, for vegetation classification, using the TIFF format images in a heterogeneous landscape is beneficial. Also, the error matrix in which overall accuracy and the kappa value signify the plot's landcover classification results (***Table 9***) shows better accuracy with TIFF images.

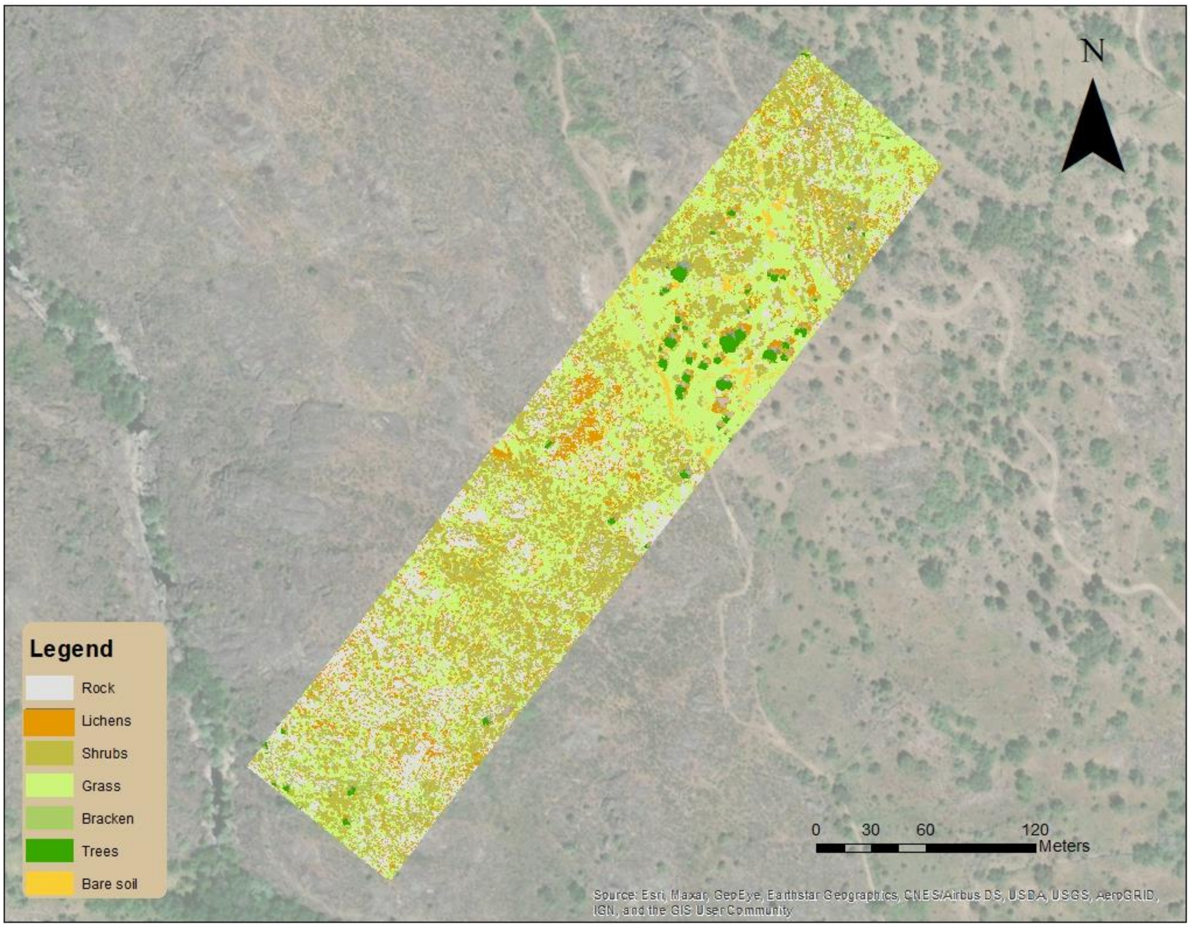

Figure 14: Map of Vale Carapito plot5 representing the vegetation classification of orthomosaic generated using TIFF images

While in the case of the error matrix generated for TIFF images, orthomosaic resulted in better accuracy with more training samples. The overall accuracy improved from 48% to 80.65%, resulting in a kappa coefficient of 0.77, as shown in *Table 9*. Lichens have the highest and bracken have the lowest producer's accuracy, while Trees and Lichens resulted with the highest user's accuracy and bracken with the lowest user's accuracy.

Table 9: Accuracy assessment of the TIFF image classification result by generating error matrix in eCognition.

Confusion Matrix (TIFF)								
User class	**Grass**	**Bracken**	**Shrubs**	**Rock**	**Trees**	**Bare soil**	**Lichens**	**Sum**
Grass	12	0	0	0	0	0	1	13
Bracken	0	2	1	0	0	0	1	4
Shrubs	2	2	15	2	2	0	0	23
Rock	1	0	3	17	1	2	0	24
Trees	0	0	0	0	14	0	0	14
Bare soil	0	0	0	1	0	8	0	9

Lichens	0	0	0	0	0	0	9	9
Sum	15	4	19	20	17	10	11	
Accuracy								
Producer	0.8	0.18	0.79	0.85	0.82	0.8	0.9	
User	0.92	0.29	0.65	0.71	1	0.89	1	
Overall Accuracy: 80.65% **Kappa: 0.77**								

The results signify that using TIFF images for the vegetation classification is better than using JPEG images. The number of training samples also plays an important role in classification. ***Figure 15*** depicts the effect of training points on the compressed and uncompressed images of orthomosaic, especially when RGB images are used.

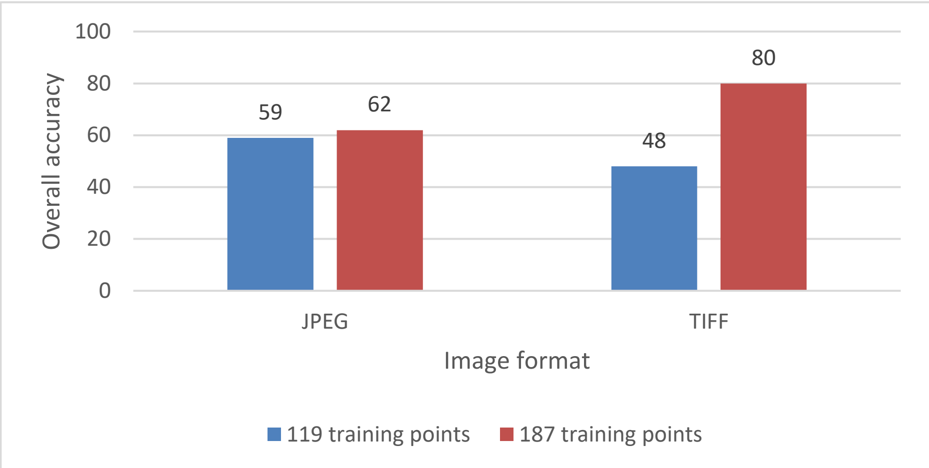

Figure 15: Bar graph with overall accuracy value of two sets of training points

3.3. Classification using Multispectral sensor

The image layer acquired from the multispectral sensor has helped improve the vegetation's segmentation and classification. The same set of training samples (187 training) was used as used for the previous research question. A canopy height model (CHM) generated using UAV-RGB was added during segmentation, as during the early spring season, deciduous trees have leaf-off conditions, and the multispectral sensor could not detect the deciduous tree structure. In contrast, the CHM of RGB orthomosaic detected the deciduous trees in the study area. The classification was visually compared with the UAV-RGB image orthomosaic, and multispectral image layers help distinguish the different vegetation types, especially between the lichens growing on the rock's surface. The trees and bare soil were best classified compared to other classes, and bracken has the lowest accuracy. Classification of the various vegetation using the multispectral sensor has shown significant results compared to RGB images. The classified map is shown in *Figure 16*, and the error matrix is in *Table 10*.

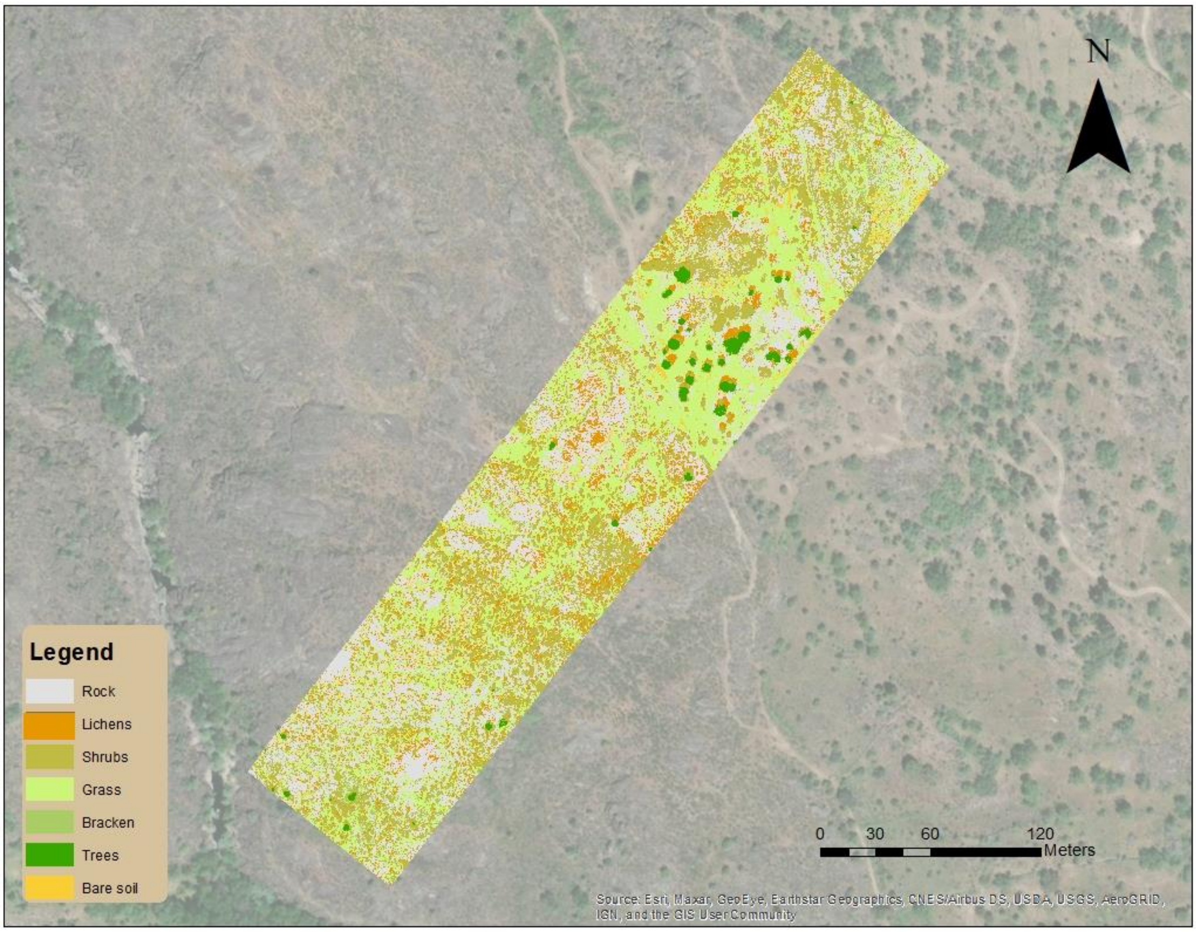

Figure 16: Map representing Vale Carapito plot5 vegetation classification of orthomosaic generated using multispectral images.

The significance of the multispectral sensor has resulted in the classification of the vegetation present in the area. The classification has resulted in 85.19% overall accuracy with a 0.83 kappa coefficient. The trees and bare soil classes have shown the highest producer's accuracy while bracken with the lowest producer's accuracy. Similarly, trees and bare soil have the highest user accuracy, and bracken has the lowest user accuracy. The error matrix has been tabulated in Table 10.

Table 10: Accuracy assessment of multispectral image classification result generated using error matrix in eCognition.

Confusion Matrix (Multispectral)								
User class	**Grass**	**Bracken**	**Shrubs**	**Rock**	**Trees**	**Bare soil**	**Lichens**	**Sum**
Grass	9	1	0	1	0	0	0	11
Bracken	0	2	1	0	0	0	0	3
Shrubs	1	0	10	0	0	0	0	11
Rock	1	1	0	7	0	0	1	10
Trees	0	0	0	0	6	0	0	6
Bare soil	0	0	0	0	0	6	0	6
Lichens	0	0	1	0	0	0	6	7
Sum	11	4	12	8	6	6	7	
Accuracy								
Producer	0.82	0.5	0.83	0.87	1	1	0.86	
User	0.82	0.66	0.90	0.73	1	1	0.85	
Overall Accuracy: 85.19% **Kappa: 0.83**								

RGB orthomosaic used different vegetation indices during segmentation and classification, while MS orthomosaic used different vegetation indices. Each layer is used by random forest classifier during creating and classifying objects. To understand the significance of each image layer with vegetation indices in classification for RGB orthomosaic and MS orthomosaic, variable importance was generated using R-studio.

Figure 17 demonstrates the image layers used for classifying RGB images using OBIA, where the Standard deviation & mean of Canopy Height Model has the highest Mean Decrease Accuracy (MDA). At the same time, similar is the case in Mean Decrease Gini (MDG). Mean Grey and mean GLI has the lowest value for Mean Decrease Accuracy and mean Grey and Standard Deviation of Blue layer have the lowest Mean Decrease Gini.

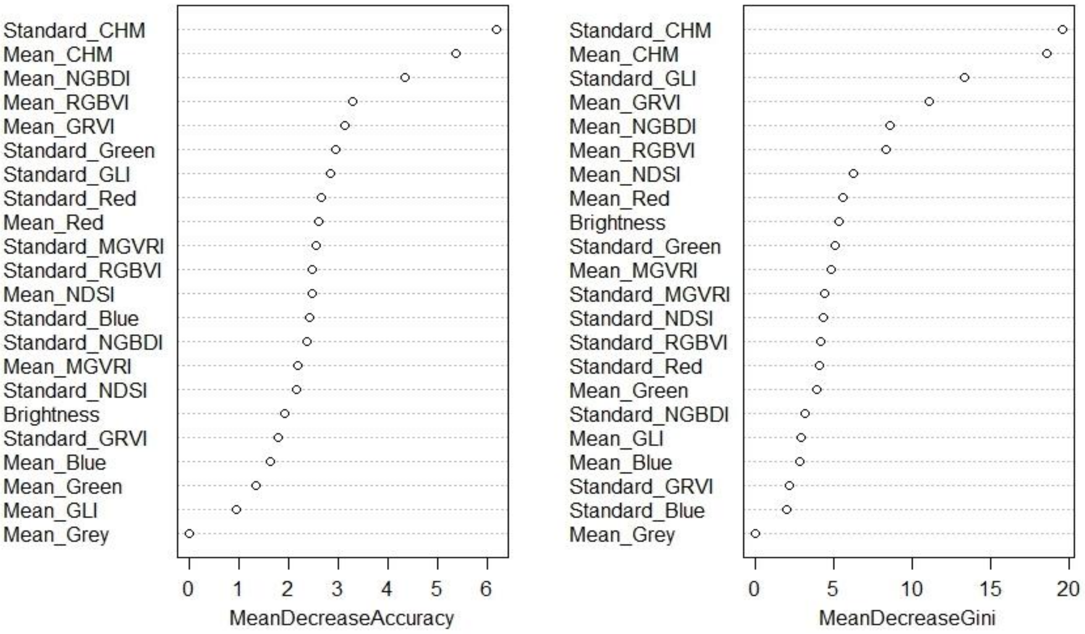

Figure 17: Variable importance plot for UAV-RGB image classification using Random Forests

As shown in ***Figure 18***, various vegetation indices were used with UAV-MS image layers for Random Forest classification. Mean NDVI has the highest Mean Decrease Accuracy, following the Mean Canopy Height Model generated using RGB and MS images. While Mean Canopy Height Model of RGB images has the

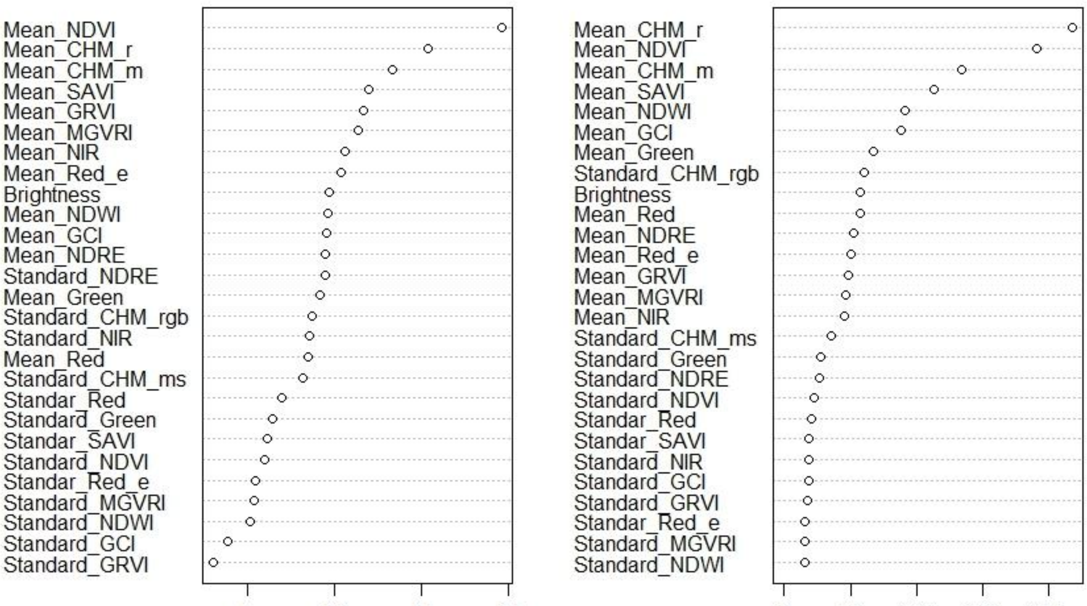

Figure 18: Variable importance plot for UAV-multispectral image classification using Random Forests

highest Mean Decrease Gini following mean NDVI and Mean CHM of MS images. The lowest Mean Decrease Accuracy is for the Standard Deviation of GRVI and GCI, whereas the standard deviation of NDWI and MGVRI has the lowest Mean Decrease of Gini.
The results signify the importance of the multispectral camera in classifying different types of vegetation compared to the RGB camera. NIR camera helps in identifying different vegetation and can distinguish rocks from lichens. NDVI plays a major role in classification also.

3.4. Significance of Ground Control Points

Ground Control Points are useful to determine the accurate measurement of X, Y, and Z values of the point of interest and to get information about the elevation of the area. They also help improve positional accuracy and reconstruction of the 3D model as it measures the value in all three directions with less error. The results of the CHM generated using GCPs and without GCPs in Vale Carapito are shown in *Figure 19*. RGB JPEG images are used for DSM and DTM generation (in two different conditions) and DSM-

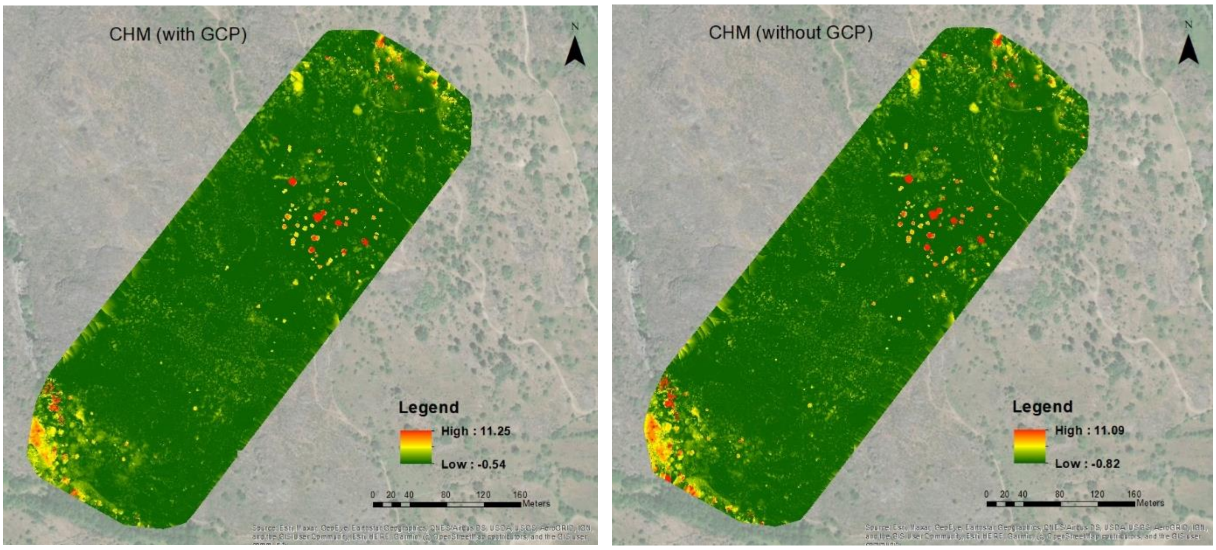

Figure 19: Canopy Height Model generated from DSM & DTM

DTM=CHM. The vegetation classification without accurate CHM is difficult for shrubs and grasses, but trees can easily be identified. The orthomosaic generated in both conditions is identical; the only difference can be seen in the positional accuracy of the field images and points. In such a landscape, where grasses and shrubs are found together, the chances of misclassification may occur, but the dominant life form is identifiable in both conditions. The raster CHM showed a different range of CHM with GCP and without GCP. So, to analyze the difference in the results of CHM, point clouds were used for analysis in two different conditions.

Point clouds co-registration of the same plot was not appropriately aligned, and cloud-to-cloud distance resulted in a mean distance of 0.20m and a standard deviation of 0.15m, while the range from 0 to 5.08m (Annex7). After ICP registration of point clouds resulted in an RMSE of 1.00158m and a transformation matrix (Annex7).

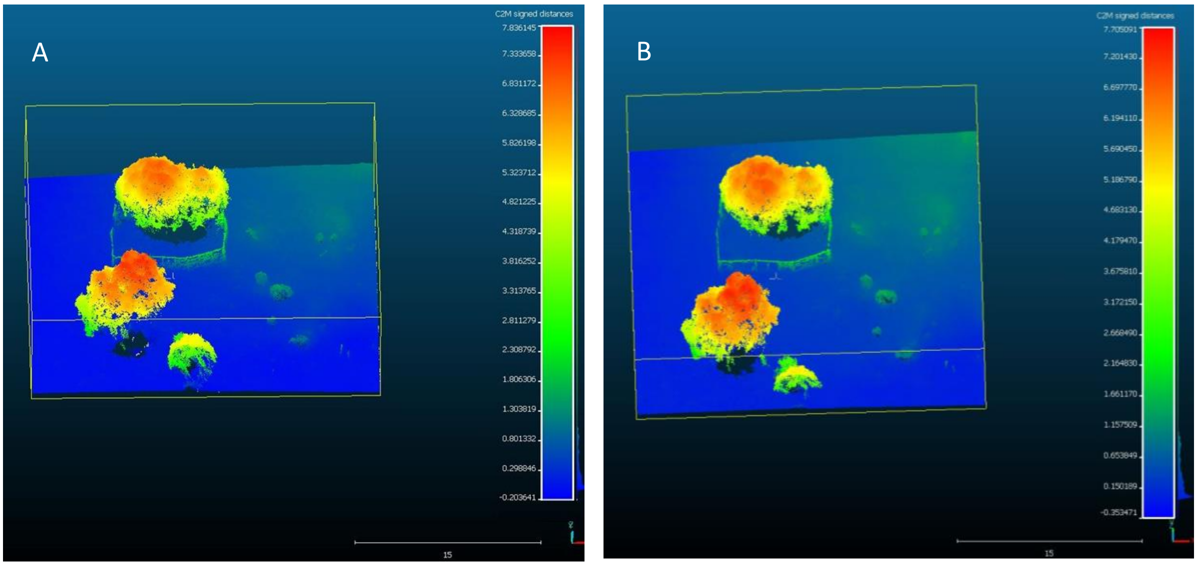

Figure 20: CHM constructed using Cloud to mesh distance in cloudcompare using point clouds generated a)with GCP and b)without GCP

A segment of the plot was used to check the height of the vegetation present, resulting in a different range of height for the same vegetation, as shown in *Figure 20*. Cloud to Mesh distance helps calculate the CHM of the vegetation in the segment. The result of Cloud to Mesh(C2M) distance computed for the segment resulted as A(point clouds generated using GCP) is from -2.03m to 7.83m. whereas Cloud to Mesh (C2M) distance computed for segment B(point clouds generated without using GCP) is from -3.5m to 7.05m.

The result shows that the range of CHM generated using point clouds for the segment is different in both cases and the highest point of the tree in case of georeferenced is higher compared to non-georeferenced. The georeferenced point cloud is expected to result in a better registration accuracy than the non-georeferenced point cloud as the GCP used to have three values which can help in better registration.

3.5. Classification of tri-seasonal orthomosaic

The combination of summer, spring, and winter orthomosaic was used for the classification, resulting in the form of a classified map, as shown in Figure 21. The vegetation classification in Figure 21 has shown high classification accuracy (92.99%). In Ermo das Águias, the area was classified into six major landcover classes: bare soil, bracken, grass, rock, shrubs, and trees. Lichens were absent in the area. The tri-seasonal orthomosaics have helped classify vegetation more accurately than a single-season orthomosaic. Accuracy in classifying the bracken in the area also improved. The trees and grass are easily distinguished in visual interpretation. The grass dominates the plot. Also, the trees have been classified quite accurately in the classified map. The distribution of the shrubs and rocks is present throughout the plot. The area has some exclusion plots demarcated to check the changes in the plot due to grazing done by the horses over time compared to the closed area. On the map, bare soil is abundant on the plot's edges due to vehicle movements for monitoring and other purposes. Therefore, it is used as a path to access the plot.

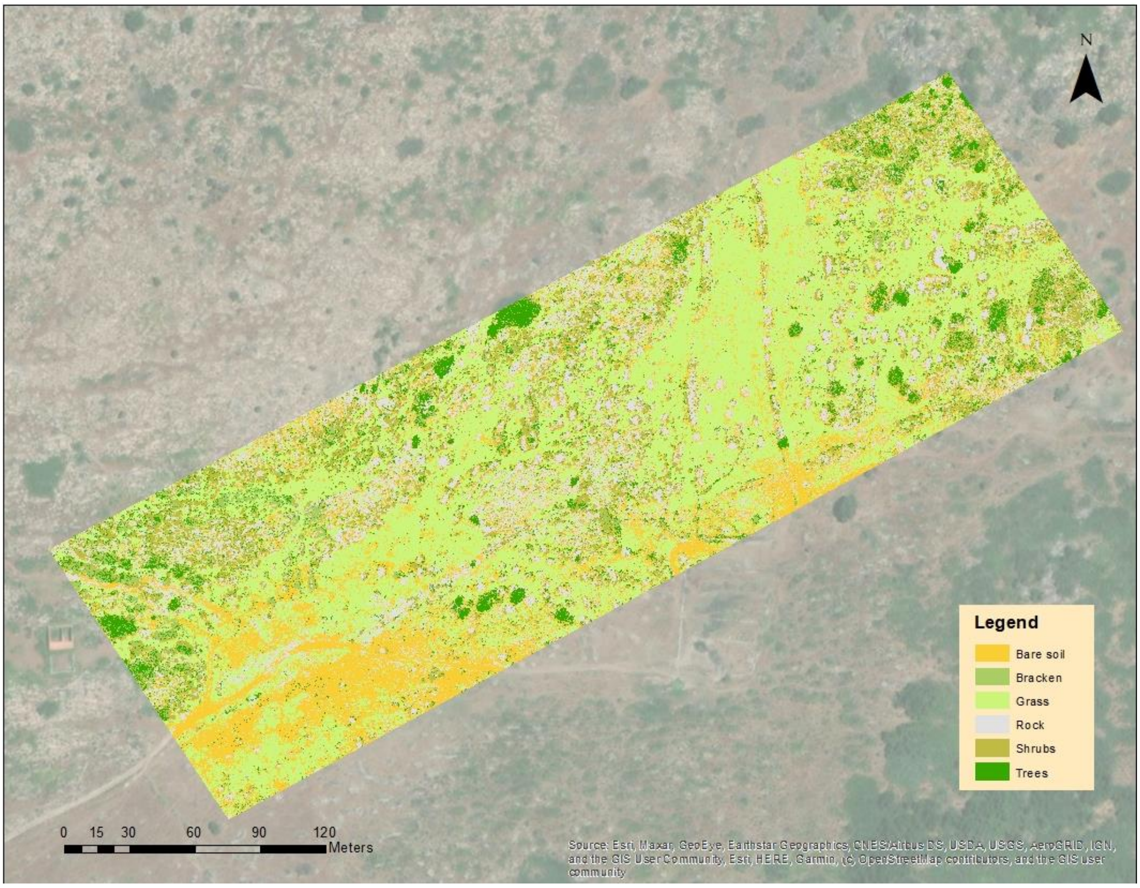

Figure 21: Map of Ermo das Águias plot5 representing the classification of combination of three-season using UAV-RGB images

Using orthomosaic of three seasons in combination to perform vegetation classification has resulted in the best results for the life-form categories. Error matrix was generated using accuracy assessment in eCognition. The classification resulted in an overall accuracy of 92.99%, with a kappa value of 0.91, as shown in Table 11. The highest producer's accuracy was shown by bare soil and the lowest of the shrubs, while in the case of user's accuracy highest was for trees and rocks, and the lowest was for the bare soil.

Table 11: Accuracy assessment of a combination of three seasons image classification in eCognition

Confusion Matrix (Three-seasons)							
User class	**Bare soil**	**Shrubs**	**Grass**	**Rock**	**Bracken**	**Trees**	**Sum**
Bare soil	28	3	1	4	0	1	37
Shrubs	0	45	0	1	0	3	49
Grass	0	0	42	0	2	0	44
Rock	0	2	0	56	0	0	58
Bracken	0	0	0	0	26	2	28
Trees	0	3	1	0	0	108	112
Sum	28	53	44	61	28	114	
Accuracy							
Producer	1	0.84	0.95	0.92	0.93	0.95	
User	0.76	0.92	0.95	0.96	0.93	0.96	
Overall Accuracy: 92.99% **Kappa: 0.911**							

As the classification involved three orthomosaic and three image layers, CHM led to much computational power to run eCognition software. So, GRVI and NDSI were used for each season to analyze the importance of vegetation indices for the classification. The variable importance (*Figure 22*) resulted in the case of classification of the combination of three seasons, using UAV-RGB images resulted in the highest Mean Decrease Accuracy of the image layer means of blue layer of winter season followed by the mean of GRVI of summer season image layer. The standard deviation of the red image layer of the spring season has the lowest. In Mean Decrease Gini, the image layer mean of a blue layer of the winter season has the highest variable importance, and the Mean of GRVI of the winter season image layer has the lowest.

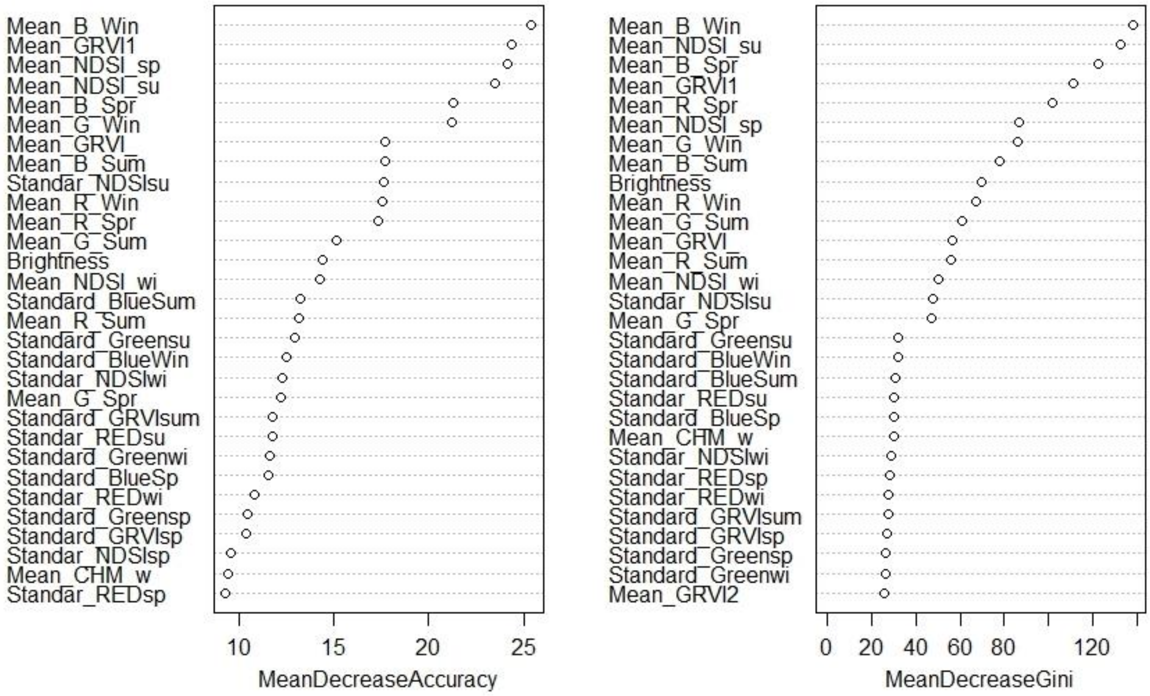

Figure 22: Variable importance plot for the combination of three seasons of UAV-RGB image classification using Random Forests.

4. DISCUSSION

4.1. Importance of Image Compression

Image compression has shown significant consequences in the results using the UAV-RGB dataset for processing and classifying RGB orthomosaic. The image format is based on the quantity and the quality of the images used. TIFF files are a lossless format, maintaining image information. On the other hand, JPEG files can be compressed at various rates (Alfio et al., 2020). JPEG imagery acquired from DJI Phantom4 was used while DNG format was changed to TIFF. The computational time and storage requirements were high when processing TIFF images, but the precision and accuracy were better than in JPEG. GCP helped to overlay the orthomosaic perfectly over each other, which can be used to compare the plot visually. There was no significant difference in orthomosaic generated with each format, and the vegetation types were easily identifiable in both cases. However, RMSE was better in the case of TIFF compared to JPEG. RMSE of TIFF for X, Y, Z is comparatively better than RMSE of JPEG, which makes TIFF format to be used for classification. Although the point cloud density of JPEG is higher, TIFF has shown better classification accuracy with the orthomosaic.

Vegetation classification with a small number of training samples resulted in poor overall accuracy and kappa with TIFF image format orthomosaic compared to JPEG image format orthomosaic. The number of training samples was increased (by adding some additional samples); this improved the classification accuracy. The classification resulted in TIFF images being classified with better accuracy and kappa value than JPEG images, as shown in *Table 8* and *Table 9*. Object-based image analysis was used with random forest for classification, which is sensitive to the image quality, the number of training samples, and parameters used for the classification (Schwind and Starek, 2017). Image format can be slightly influenced by the form of the ground's surface (terrain of the ground), the sensors and the platform used for the data acquisition. The images acquired in the summer of 2021 were in TIFF and JPEG format. The first flight did not include raw images, and the whole area was not covered, so the second flight with raw and jpeg images was planned. The orthomosaic generated using the images was not properly aligned to each other. There was a slight shift in the orthomosaic due to the images saved in the card during acquisition or the platform used.

It also plays importance in the creation of point cloud density which further helps intensify the vertical information and 3D structure of the vegetation, which can be used as a baseline for the comparison.

4.2. Role of GCPs in image classification

CHM is useful in vegetation classification and helps determine the vegetation structure and plant life forms. To understand the importance of GCP, two projects created with JPEG images, one with GCP and the other without GCP, resulted in orthomosaic, DSM, and DTM. The orthomosaic was similar but was not aligned because orthomosaic with no GCP will use the georeferencing from UAV-RGB images and will not be as accurate and precise as GNSS measurements. Also, the results of SfM processing resulted in DSM and DTM being used to generate the Canopy Height Model.

The significance of CHM in vegetation classification was evident in the UAV-RGB and UAV-MS classification, in which CHM have shown as an essential variable for improving accuracy (as in *Figure 17* and *Figure 18*). Some studies show that DTM is affected by the ground points, and GCP helps correct DTM & DSM values, which helps achieve better accuracy for CHM (Awasthi et al., 2020; Gindraux et al., 2017). Thus, the accurate measurement helps in forming an accurate representation of the area, which can be used by the user for future reference or to monitor the changes in the area.

After generating an orthomosaic with different conditions but the same images resulted in a different range of CHM. However, the vegetation classification with the same training samples will give different results due to the shift in data. Training points do not align with the shape of the objects in case of not georeferenced orthomosaic. So, Point clouds were used to answer the research question about the importance of GCP in determining vegetation structure. Point clouds are one of the results of SfM processing and help create a 3D structure of the area or an object. The point clouds density is essential as it gives more data about the area and helps in classification. JPEG has resulted in a high point cloud density compared to TIFF images point cloud density, which was used for further study. As the manual fine registration is not possible for the vegetation, which is not uniform from each side, so fine ICP registration was used. The higher RMSE of point cloud registration attributes to the poor alignment between the point clouds. Point clouds were useful to identify the presence of different plant life forms, especially trees and shrubs. Grasses were small and could not be distinguished properly, although artificial objects like fencing and borders having certain heights could show in 3D structure.

A segment in the plot was used to check if the presence and absence of GCP help in accurate estimation of the vegetation structure or height, and the same vegetation was compared. CHM resulted in two conditions, giving in a difference of 80cm between the tree's highest point in the segment, as shown in *Figure 20*. The ground data is important for accurate vertical information of the vegetation. Improving the vegetation structure's accuracy for comparison in future GCP is important and influences the results of photogrammetric processing (Awasthi et al., 2020).

Point clouds were useful in generating the structure of the trees and shrubs. By using the present point cloud data to compare the future conditions of trees and shrubs can help monitor the vegetation change in the area. It will help the team understand the changes happening in the area and decide the management strategies. So, GCP is essential to compare the changes over a period of time, but if it is necessary to classify the area into different landcover for maps, then it can be done without GCP but will not be helpful for future comparisons.

4.3. Effect of VNIR multiple data

For the study, UAV-RGB and UAV-MS imageries were processed and classified based on the life-form classes identified. Different vegetation indices were generated using UAV-RGB images and UAV-MS images. Visible and Near-infrared (VNIR) multispectral data is useful for identifying different life-form classes. Ashapure et al., (2019) signified the importance of multispectral sensors in accurately estimating canopy cover model with respect to RGB-based datasets. NDVI has played an important role in improving classification accuracy.

The RGB orthomosaic was generated using TIFF images with three image layers (Red, Green, and Blue). For classification, CHM generated was added as the image layer along with other vegetation indices (*Table 4*), which helped improve segmentation and classification. Prošek and Šímová, (2019a) compared the multispectral & multispectral with SfM processing, which resulted in a viable method for mapping shrubland, which is a similar case to the heterogeneous landscape taken as a study area. The research justifies that the fusion of multispectral with SfM has resulted in better results in classifying different classes compared to RGB orthomosaic. CHM helps in differentiating the vegetation based on height. The CHM of multispectral images was not identifying the presence of deciduous trees. As the images acquired were of leaf-off season, the sensor captured images directly on land. In comparison, CHM of RGB imagery detected the presence of deciduous trees in the area.

The classification resulted in an overall accuracy of 80.65% and a 0.77 kappa value as in *Table 9*. The variable importance helped in understanding which image layer has shown the high significance in classifying the image layer. CHM has shown the highest importance in Mean Decrease Accuracy and Mean Decrease Gini (*Figure 17*). CHM has played an important role in classifying different vegetation types using OBIA, while Mean GLI has the least important role in improving the classification accuracy.

In the case of Multispectral image classification, four different image layers were acquired from four different cameras of Parrot Sequoia (Green, Red, NIR, Red-edge). The combination of four image layers was used along with CHM generated using MS and RGB images. RGB image of parrot sequoia was not used as DJI camera is better. CHM generated from UAV-RGB images was added because the deciduous trees in the region were in leaf-off condition, and the sensor could not correctly distinguish the tree structure from the ground. The coarse resolution of the sensor made it more difficult. So, in order to distinguish and correctly classify the deciduous trees, UAV-RGB generated CHM was added during OBIA in eCognition. The vegetation indices used for multispectral imageries classification differed from those used for RGB image classification, as shown in *Table 5*. Vegetation indices generated using multispectral sensors have helped improve the classification accuracy, and the NIR image layer has shown significant importance in the classification, as seen in the variable importance *Figure 18*. The variable importance graph of Mean Decrease Accuracy has signified mean NDVI's importance in improving classification accuracy, followed by mean CHM using UAV-RGB images and UAV-MS images. While Standard deviation GRVI and GCI have minor importance. The error matrix generated resulted in an overall accuracy of 85.19% and a kappa value of 0.83 (*Table 10*).

The multispectral sensor has dedicated sensors extending to the near-infrared wavelength with different spectral resolutions, and calibration of the UAV acquired imageries during SfM processing helps distinguish different vegetation present on the ground. *Table 10* shows the highest user and producer accuracy of the bare soil and trees, in which the NIR image layer and NDVI have shown a high significance. The area has a high presence of grass, rocks, and shrubs, and sometimes it is hard to distinguish between the vegetation classes based on the height. The spectral value of each vegetation is different, which helps identify the different types of vegetation present in the area, especially between bare soil - grass & rock - lichens. The presence of lichens is quite correctly classified with multispectral imageries and RGB image classifications, but rock classification slightly improved in the case of multispectral classification. The lichens were dried and burnt (as sown in *Figure 23*) due to fire and drought conditions in the region; they looked similar to rocks in RGB images. So, the multispectral sensor helped in distinguishing the rock and lichens.

Figure 23: Image showing a) the dried lichens grown on the surface of the rock in Vale Carapito b) Dried lichens on the rock surface and a patch of deciduous trees in Vale Carapito

Further, the classification accuracy of shrubs and bracken improved with the multispectral image classification. The different phenological characteristics of plants have been used to distinguish the species with the help of multispectral images (Paz-Kagan et al., 2019), and this is evident in the results of the error matrix of the multispectral image classification *Table 10*. During winter season, bracken was dried and was not easily identifiable from the orthomosaic but shrubs were in flowering condition and was quite evident in the images. The segments were easily constructed with multispectral images and resulted in good classification accuracy. An image of the area covered with shrubs (white flowers in bloom) from the field site is shown in *Figure 24*.

Figure 24: Dense patch of white broom shrubs in bloom in Vale Carapito

4.4. Effect of multiple seasons data on vegetation classification

Various studies have signified the importance of season in improving classification accuracy (Chib, 2021; J. Liu et al., 2015; Macintyre et al., 2020). The combination of seasons for the classification has resulted in a high accuracy compared to other classifications *Table 11*. The classification was done using UAV-RGB images, and it was evident to observe the changes in the phenology of vegetation present in the area.

The winter season orthomosaic shows the prominent presence of shrubs as they were flowering and perennial trees and deciduous trees difference was easily identifiable. In visual comparison of the orthomosaic, there were changes found in the shrubs as there was a time difference of an year between the image acquisition. Grass was prominent in the winter and spring orthomosaic. The presence of bracken is hard to distinguish in the winter orthomosaic but it was evident in summer and spring orthomosaic. The difference in phenology of vegetation can be seen in *Figure 25*.

Figure 25: Screenshot of three seasons (spring, summer, and winter) covered with shrubs, bracken, grass, and rocks

A high overall accuracy of 92.99% was resulted using error matrix and 0.91 kappa value. Grass and trees have given the best results, whereas bracken was classified quite accurately and resulted in high accuracy (user and producer accuracy = 0.93). *Figure 25* shows the change in the colour of bracken in each season, and the various seasonal image layer improved its segmentation and classification. The early spring (March 2022) orthomosaic was useful in distinguishing between deciduous and perennial trees; under canopy vegetation for deciduous trees was visible in UAV images. The white broom shrubs were in the blooming stage, which helped in distinguishing them easily. The grass was greener compared to summer orthomosaic while it was on the growing stage for spring. Whereas it was difficult to distinguish between lichens and rock, bracken was hard to identify in RGB orthomosaic. Bracken (yellowish-green in color) was easily identified in summer orthomosaic.

Vegetation indices (NDSI and GRVI) was generated of each season to improve the segmentation and classification of the combined imageries. The variable importance in *Figure 22* of combined season shows the highest importance of Mean Blue image layer of winter while standard deviation of Red image layer of spring season as the lowest for Mean Decrease Accuracy. While, mean blue image layer of winter season have the highest, and mean GRVI of winter imagery has the lowest Mean Decrease Gini. The significance of the March 2022 orthomosaic is evident in classifying the shrubs and trees. Bare soil is quite evident in the summer and spring orthomosaic, and the high presence of bare soil on the edges shows the significance of each season's image layer. The CHM of winter imagery was used to segment and classify the orthomosaic, but it has shown less significance in the variable importance graph. Each season's variation in the different vegetation improves the classification accuracy (J. Liu et al., 2015).

During the processing of the OBIA, the orthomosaics of three seasons were not correctly aligned because different drone and flight parameters were used for image acquisition, resulting in different ground sampling distances. The absolute accuracy of UAV-GPS led to some errors, reflected in the orthomosaics. So, to align different orthomosaics decently, multi-tie points were used. The results address the importance of GCP in accurately aligning multi seasons images so they can be used for future purposes.

4.5. Comparison of results

Comparing the results of TIFF-RGB and JPEG-RGB signifies the importance of the image quality and the data stored in each imagery. Uncompressed (TIFF) imagery has given better results with reasonable accuracy but requires more processing time, computational power, and storage. So, it depends on the use and purpose of the user to decide the image format to be used for vegetation classification. To use the results in the future, it is better to use TIFF format images for the vegetation classification and generate high-quality results.

Between UAV-RGB and UAV-MS, classification accuracy improved in the case of multispectral but with a 5% difference in overall accuracy, but classification in each class was much better compared to RGB. The considerable advantage of multispectral classification was the low effect of shadow during segmentation and classification; as in the case of RGB images, the shadows and GCP target marks were segmented as objects, which hamper the classification of the vegetation, especially in the case of trees and high shrubs. The sensor is useful for identifying the vegetation types at the species level, but to classify vegetation at a dominant level, a UAV-RGB camera can be considered sufficient.

To compare the results of GCP and without GCP, it is evident to use GCP for positional accuracy in results and to use the classified maps for future reference. It is difficult to overlay the orthomosaic acquired during different time periods and compare with it. GCP-generated vegetation structure determines an accurate vegetation structure and CHM. This will be helpful in comparing the change in the vegetation structure with the period of time.

In comparing using single-season orthomosaic, the combination of different season orthomosaic has given a better classification and high overall accuracy and kappa value. So, to align multiple seasons orthomosaic for comparison or classification, GCPs are essential. Using single-season orthomosaic for classification has resulted in classifying some of the life-form categories to be accurately classified but have misclassified between grass, shrubs and bracken, which are found in the area. The combination of the seasons has significantly contributed to the classification and is demonstrated in *Figure 21*.

4.6. Application of the results

The results generated from this study are helpful for conservation organizations like Rewilding Portugal. Furthermore, the efforts to rewild other areas in Europe are intensifying, for example, Rewilding Europe sites. This study compared instruments, platforms, and methods to classify vegetation. These results serve as the baseline for vegetation monitoring in the Côa Valley and formalize an efficient, low-cost protocol to be used in monitoring other ecosystems. UAV imageries are high-resolution data, and processing them requires high computational power and systems. The study was applied on the ground level to understand the importance of detailed and accurate imagery for planning, monitoring, and conserving the area. The maps generated on the plant life-form categories will help to understand the distribution of the vegetation types in the area and to further work on the detailed level for the comparison of types of species present in the area.

Using the same method for the classification and for different dataset have resulted in good accuracy with the combination of three-seasons. This can be useful for monitoring, understanding the vegetation dynamics of the region, and understanding the heterogeneity landscape in the presence of the grazing animals.

4.7. Limitations in the study

- GCP was only acquired during one season, and it is difficult to combine several images of the same area acquired at different times. The GCP helps in overlaying the imageries accurately and precisely, which can be used for the comparison and analysis in the future.

- The number of samples for bracken and bare soil were less compared to other land covers. The seasonal change was evident in case of bracken and bare soil. During spring, bare soil have small patches in the plot but during summer grass area was dry and looks bare.

- Due to high computational processing power required in eCognition software Estimation of scale parameter (ESP) tool could not be used. Trial and error method was used for segmentation during OBIA.

5. CONCLUSION AND RECOMMENDATION

5.1. Conclusions

The study investigates the low-cost method for the vegetation classification of the area by comparing the different sensors, image formats, and seasonality using the same method for classification, OBIA. The study has shown that the vegetation classification method is helpful and can be used in various conditions and regions. The main aim was to improve the classification of accuracy of the vegetation classification and for which TIFF image format (overall 80%) has given a good accuracy compared to JPEG(overall 65%). With the increase in training points, classification accuracy improved. This resulted in the random forest classifier being sensitive to the number of training points. The classification accuracy of multispectral image orthomosaic (overall accuracy 85%) is significantly better than RGB orthomosaic (overall accuracy 80%). The presence of visible and near-infrared images helps in better identification and spectrally differentiating species for classification, improving the accuracy of the lichens, rock, bare soil, and shrubs. However, it depends on the aim with which the classification is to be done because a multispectral sensor can be costly in comparison to a UAV-RGB sensor. It is evident that GCP has to be used for the area's classification and future purposes. GCP will help properly align multi-season images, which can help achieve the vegetation classification.

The research showed that combining three-season orthomosaic will give the highest classification accuracy compared to single-season or multispectral. The overall accuracy was 93%, and TIFF-RGB images were used for the classification. If the data can be collected at different seasons and without much cost and effort, then a combination of seasons is the best approach for heterogeneous landscape vegetation classification. Also, early spring or late winter time has resulted useful in differentiating plant life forms. So, for better alignment, GCPs are necessary. In case if one-time data acquisition is done and classifies the vegetation, then a multispectral sensor will be helpful. For object-based image analysis (OBIA), eCognition is the best tool, but using this software with TIFF image formats for classifications requires high storage capacity and a good computational power system. In a nutshell, the research results will be helpful and efficient in vegetation monitoring using low-cost methods in other ecosystems for conservation and monitoring purposes.

5.2. Recommendations for further studies

For future studies, GCPs are useful for the comparison of multi-temporal imageries. It will be beneficial to fix a few permanent marks in the area, which can be used as GCP to overlay orthomosaic of different times or seasons. This will be useful for classification at the species level, which can be an important step to improving and understanding the vegetation dynamics of the existing species in the area. For species identification, vegetation indices are helpful. So, for vegetation classification, using vegetation indices Jeong et al., (2018), suggested the use of calibrated RGB images to generate vegetation indices based on the reflectance value. The results of such a study can be new and beneficial for further research. Also, the illumination conditions are dynamic in any study area. So, further study or research with calibration panels for RGB images should be used to find the difference in classification accuracy.

The usefulness of SfM processing is that point clouds can help detect the changes in vegetation classification. Point clouds will help generate 3D structures which can easily be used for trees, shrubs or artificial objects with height. Cloudcompare software can be considered useful for such comparisons in the future, as eCognition is a licensed software while cloudcompare is free and open to access.

6. LIST OF REFERENCES

Aasen, H., Honkavaara, E., Lucieer, A., Zarco-Tejada, P.J., 2018. Quantitative remote sensing at ultra-high resolution with UAV spectroscopy: A review of sensor technology, measurement procedures, and data correctionworkflows. Remote Sens. 10, 1–42. https://doi.org/10.3390/rs10071091

Accuracy metrics [WWW Document], n.d. URL http://gsp.humboldt.edu/olm/Courses/GSP_216/lessons/accuracy/metrics.html

Agüera-Vega, F., Carvajal-Ramírez, F., Martínez-Carricondo, P., 2017a. Assessment of photogrammetric mapping accuracy based on variation ground control points number using unmanned aerial vehicle. Meas. J. Int. Meas. Confed. 98, 221–227. https://doi.org/10.1016/j.measurement.2016.12.002

Agüera-Vega, F., Carvajal-Ramírez, F., Martínez-Carricondo, P., 2017b. Assessment of photogrammetric mapping accuracy based on variation ground control points number using unmanned aerial vehicle. Measurement 98, 221–227. https://doi.org/10.1016/J.MEASUREMENT.2016.12.002

Alfio, V.S., Costantino, D., Pepe, M., 2020. Influence of image tiff format and jpeg compression level in the accuracy of the 3d model and quality of the orthophoto in uav photogrammetry. J. Imaging 6. https://doi.org/10.3390/jimaging6050030

Alvarez-Vanhard, E., Houet, T., Mony, C., Lecoq, L., Corpetti, T., 2020. Can UAVs fill the gap between in situ surveys and satellites for habitat mapping? Remote Sens. Environ. 243, 111780. https://doi.org/10.1016/j.rse.2020.111780

Ashapure, A., Jung, J., Chang, A., Oh, S., Maeda, M., Landivar, J., 2019. A comparative study of RGB and multispectral sensor-based cotton canopy cover modelling using multi-temporal UAS data. Remote Sens. 11. https://doi.org/10.3390/rs11232757

Awasthi, B., Karki, S., Regmi, P., Dhami, D.S., Thapa, S., Panday, U.S., 2020. Analyzing the effect of distribution pattern and number of GCPs on overall accuracy of UAV photogrammetric results. Lect. Notes Civ. Eng. 51, 339–354. https://doi.org/10.1007/978-3-030-37393-1_29

Baena, S., Moat, J., Whaley, O., Boyd, D.S., 2017. Identifying species from the air: UAVs and the very high resolution challenge for plant conservation. PLoS One 12, 1–21. https://doi.org/10.1371/journal.pone.0188714

Baxendale, C.L., Ostle, N.J., Wood, C.M., Oakley, S., Ward, S.E., 2016. Can digital image classification be used as a standardised method for surveying peatland vegetation cover? Ecol. Indic. 68, 150–156. https://doi.org/10.1016/J.ECOLIND.2015.11.035

Belgiu, M., Drăgu, L., 2016. Random forest in remote sensing: A review of applications and future directions. ISPRS J. Photogramm. Remote Sens. 114, 24–31. https://doi.org/10.1016/j.isprsjprs.2016.01.011

Bendig, J., Yu, K., Aasen, H., Bolten, A., Bennertz, S., Broscheit, J., Gnyp, M.L., Bareth, G., 2015. Combining UAV-based plant height from crop surface models, visible, and near infrared vegetation indices for biomass monitoring in barley. Int. J. Appl. Earth Obs. Geoinf. 39, 79–87. https://doi.org/10.1016/J.JAG.2015.02.012

Berra, E.F., Gaulton, R., Barr, S., 2019. Assessing spring phenology of a temperate woodland: A multiscale comparison of ground, unmanned aerial vehicle and Landsat satellite observations. Remote Sens. Environ. 223, 229–242. https://doi.org/10.1016/j.rse.2019.01.010

Candiago, S., Remondino, F., De Giglio, M., Dubbini, M., Gattelli, M., Lucieer, A., Zarco-Tejada, P.J., Rascher, U., Bareth, G., Inoue, Y., Thenkabail, P.S., 2015. Evaluating Multispectral Images and Vegetation Indices for Precision Farming Applications from UAV Images. Remote Sens. 2015, Vol. 7, Pages 4026-4047 7, 4026–4047. https://doi.org/10.3390/RS70404026

Chen, F., Van de Voorde, T., Roberts, D., Zhao, H., Chen, J., 2021. Detection of ground materials using normalized difference indices with a threshold: Risk and ways to improve. Remote Sens. 13, 1–10. https://doi.org/10.3390/rs13030450

Chen, Y., Chen, Q., Jing, C., 2021. Multi-resolution segmentation parameters optimization and evaluation for VHR remote sensing image based on meanNSQI and discrepancy measure. J. Spat. Sci. 66, 253–278. https://doi.org/10.1080/14498596.2019.1615011

Chib, R.S., 2021. Drones for conservation: Integrating UAVs with field methods to classify satellite imagery to map plant communities-A case study of Drentsche AA, The Netherlands.

Cloudcompare forum [WWW Document], n.d. URL https://cloudcompare.org/forum/viewtopic.php?t=4624 (accessed 4.10.22).

Copernicus, 2018. Corine Land Cover 2018 [WWW Document]. URL https://land.copernicus.eu/pan-european/corine-land-cover/clc2018

Crommelinck, S., Bennett, R., Gerke, M., Yang, M.Y., Vosselman, G., 2017. Contour detection for UAV-based cadastral mapping. Remote Sens. 9, 1–13. https://doi.org/10.3390/rs9020171

D'Urso, M.G., Rotondi, A., Gagliardini, M., 2018. UAV low-cost system for evaluating and monitoring the growth parameters of crops. ISPRS Ann. Photogramm. Remote Sens. Spat. Inf. Sci. 4, 405–413. https://doi.org/10.5194/isprs-annals-IV-5-405-2018

DeSilvey, C., Bartolini, N., 2019. Where horses run free? Autonomy, temporality and rewilding in the Côa Valley, Portugal. Trans. Inst. Br. Geogr. 44, 94–109. https://doi.org/10.1111/TRAN.12251/FORMAT/PDF

Du, M., Noguchi, N., 2017. Monitoring of wheat growth status and mapping of wheat yield's within-field spatial variations using color images acquired from UAV-camera System. Remote Sens. 9. https://doi.org/10.3390/rs9030289

Fuentes-Peailillo, F., Ortega-Farias, S., Rivera, M., Bardeen, M., Moreno, M., 2019. Comparison of vegetation indices acquired from RGB and Multispectral sensors placed on UAV. IEEE ICA-ACCA 2018 - IEEE Int. Conf. Autom. Congr. Chil. Assoc. Autom. Control Towar. an Ind. 4.0 - Proc. https://doi.org/10.1109/ICA-ACCA.2018.8609861

Furukawa, F., Laneng, L.A., Ando, H., Yoshimura, N., Kaneko, M., Morimoto, J., 2021. Comparison of rgb and multispectral unmanned aerial vehicle for monitoring vegetation coverage changes on a landslide area. Drones 5. https://doi.org/10.3390/drones5030097

García-Fernández, M., Sanz-Ablanedo, E., Rodríguez-Pérez, J.R., 2021. High-resolution drone-acquired RGB imagery to estimate spatial grape quality variability. Agronomy 11. https://doi.org/10.3390/agronomy11040655

Gerke, M., Przybilla, H.J., 2016. Accuracy analysis of photogrammetric UAV image blocks: Influence of onboard RTK-GNSS and cross flight patterns. Photogramm. Fernerkundung, Geoinf. 2016, 17–30. https://doi.org/10.1127/pfg/2016/0284

Gindraux, S., Boesch, R., Farinotti, D., 2017. Accuracy assessment of digital surface models from Unmanned Aerial Vehicles' imagery on glaciers. Remote Sens. 9, 1–15. https://doi.org/10.3390/rs9020186

Grybas, H., Congalton, R.G., 2021. A comparison of multi-temporal rgb and multispectral uas imagery for tree species classification in heterogeneous new hampshire forests. Remote Sens. 13. https://doi.org/10.3390/rs13132631

Heywood, V.H., Iriondo, J.M., 2003. Plant conservation: Old problems, new perspectives. Biol. Conserv. 113, 321–335. https://doi.org/10.1016/S0006-3207(03)00121-6

How to generate point cloud classification [WWW Document], 2022. . Pix4D. URL https://support.pix4d.com/hc/en-us/articles/115004864586-How-to-generate-the-point-cloud-classification#label1

Huete, A.R., 1988. A soil-adjusted vegetation index (SAVI). Remote Sens. Environ. 25, 295–309. https://doi.org/10.1016/0034-4257(88)90106-X

Jeong, Y., Yu, J., Wang, L., Shin, H., Koh, S.M., Park, G., 2018. Cost-effective reflectance calibration method for small UAV images. Int. J. Remote Sens. 39, 7225–7250. https://doi.org/10.1080/01431161.2018.1516307

Joffre, R., Rambal, S., 2001. Mediterranean Ecosystems. eLS. https://doi.org/10.1038/NPG.ELS.0003196

Johnson, B.A., Ma, L., 2020. Image segmentation and object-based image analysis for environmental monitoring: Recent areas of interest, researchers' views on the future priorities. Remote Sens. 12. https://doi.org/10.3390/rs12111772

Johnston, D.W., 2019. Unoccupied aircraft systems in marine science and conservation. Ann. Rev. Mar. Sci. 11, 439–463. https://doi.org/10.1146/annurev-marine-010318-095323

Kamagata, N., Hara, K., Mori, M., Akamatsu, Y., Li, Y., Hoshino, Y., 2006. A new method of vegetation mapping by object-based classification using high resolution satellite data. J. Japan Soc. Photogramm. Remote Sens. 45, 43–49. https://doi.org/10.4287/JSPRS.45.43

Kaneko, K., Nohara, S., 2014. Review of Effective Vegetation Mapping Using the UAV (Unmanned Aerial Vehicle) Method. J. Geogr. Inf. Syst. 06, 733–742. https://doi.org/10.4236/jgis.2014.66060

Kattenborn, T., Eichel, J., Fassnacht, F.E., 2019. Convolutional Neural Networks enable efficient, accurate and fine-grained segmentation of plant species and communities from high-resolution UAV imagery. Sci. Rep. 9, 1–9. https://doi.org/10.1038/s41598-019-53797-9

Kent, M., 2012. Vegetation Description and Data Analysis 438.

Liang, W., Abidi, M., Carrasco, L., McNelis, J., Tran, L., Li, Y., Grant, J., Liang, W., 2020. Mapping vegetation at species level with high-resolution multispectral and lidar data over a large spatial area: A case study with Kudzu. Remote Sens. 12. https://doi.org/10.3390/rs12040609

Liu, J., Heiskanen, J., Aynekulu, E., Pellikka, P.K.E., 2015. Seasonal variation of land cover classification accuracy of Landsat 8 images in Burkina Faso. Int. Arch. Photogramm. Remote Sens. Spat. Inf. Sci. - ISPRS Arch. 40, 455–460. https://doi.org/10.5194/isprsarchives-XL-7-W3-455-2015

Liu, Jing, Li, P., Wang, X., 2015. A new segmentation method for very high resolution imagery using spectral and morphological information. ISPRS J. Photogramm. Remote Sens. 101, 145–162. https://doi.org/10.1016/j.isprsjprs.2014.11.009

Liu, M., Yu, T., Gu, X., Sun, Z., Yang, J., Zhang, Z., Mi, X., Cao, W., Li, J., 2020. The impact of spatial resolution on the classification of vegetation types in highly fragmented planting areas based on unmanned aerial vehicle hyperspectral images. Remote Sens. 12. https://doi.org/10.3390/RS12010146

López, J.J., Mulero-Pázmány, M., 2019. Drones for conservation in protected areas: Present and future. Drones 3,

1–23. https://doi.org/10.3390/drones3010010
Lussem, U., Bolten, A., Gnyp, M.L., Jasper, J., Bareth, G., 2018. Evaluation of RGB-based vegetation indices from UAV imagery to estimate forage yield in Grassland. Int. Arch. Photogramm. Remote Sens. Spat. Inf. Sci. - ISPRS Arch. 42, 1215–1219. https://doi.org/10.5194/isprs-archives-XLII-3-1215-2018
Macintyre, P., van Niekerk, A., Mucina, L., 2020. Efficacy of multi-season Sentinel-2 imagery for compositional vegetation classification. Int. J. Appl. Earth Obs. Geoinf. 85, 101980. https://doi.org/10.1016/j.jag.2019.101980
Makinde, E.O., Salami, A.T., Olaleye, J.B., Okewusi, O.C., 2016. Object Based and Pixel Based Classification Using Rapideye Satellite Imager of ETI-OSA, Lagos, Nigeria. Geoinformatics FCE CTU 15, 59–70. https://doi.org/10.14311/gi.15.2.5
Manfreda, S., McCabe, M.F., Miller, P.E., Lucas, R., Madrigal, V.P., Mallinis, G., Dor, E. Ben, Helman, D., Estes, L., Ciraolo, G., Müllerová, J., Tauro, F., de Lima, M.I., de Lima, J.L.M.P., Maltese, A., Frances, F., Caylor, K., Kohv, M., Perks, M., Ruiz-Pérez, G., Su, Z., Vico, G., Toth, B., 2018. On the use of unmanned aerial systems for environmental monitoring. Remote Sens. 10. https://doi.org/10.3390/rs10040641
Martínez-Carricondo, P., Agüera-Vega, F., Carvajal-Ramírez, F., Mesas-Carrascosa, F.J., García-Ferrer, A., Pérez-Porras, F.J., 2018. Assessment of UAV-photogrammetric mapping accuracy based on variation of ground control points. Int. J. Appl. Earth Obs. Geoinf. 72, 1–10. https://doi.org/10.1016/j.jag.2018.05.015
Matese, A., Di Gennaro, S.F., Berton, A., 2016. Assessment of a canopy height model (CHM) in a vineyard using UAV-based multispectral imaging. https://doi.org/10.1080/01431161.2016.1226002 38, 2150–2160. https://doi.org/10.1080/01431161.2016.1226002
Millard, K., Richardson, M., 2015. On the importance of training data sample selection in Random Forest image classification: A case study in peatland ecosystem mapping. Remote Sens. 7, 8489–8515. https://doi.org/10.3390/rs70708489
Mlambo, R., Woodhouse, I.H., Gerard, F., Anderson, K., 2017. Structure from motion (SfM) photogrammetry with drone data: A low cost method for monitoring greenhouse gas emissions from forests in developing countries. Forests 8, 68. https://doi.org/10.3390/f8030068
Morgan, J.L., Gergel, S.E., Coops, N.C., 2010. Aerial Photography: A Rapidly Evolving Tool for Ecological Management. Bioscience 60, 47–59. https://doi.org/10.1525/BIO.2010.60.1.9
Motzkin, G., Wilson, P., Foster, D.R., Allen, A., 1999. Vegetation patterns in heterogeneous landscapes: The importance of history and environment. J. Veg. Sci. 10, 903–920. https://doi.org/10.2307/3237315
Müllerová, J., Bartaloš, T., Brůna, J., Dvořák, P., Vítková, M., 2017. Unmanned aircraft in nature conservation: an example from plant invasions. Int. J. Remote Sens. 38, 2177–2198. https://doi.org/10.1080/01431161.2016.1275059
Müllerová, J., Gago, X., Bučas, M., Company, J., Estrany, J., Fortesa, J., Manfreda, S., Michez, A., Mokroš, M., Paulus, G., Tiškus, E., Tsiafouli, M.A., Kent, R., 2021. Characterizing vegetation complexity with unmanned aerial systems (UAS) – A framework and synthesis. Ecol. Indic. 131. https://doi.org/10.1016/j.ecolind.2021.108156
Munyati, C., 2018. Optimising multiresolution segmentation: Delineating savannah vegetation boundaries in the Kruger National Park, South Africa, using Sentinel 2 MSI imagery. Int. J. Remote Sens. 39, 5997–6019. https://doi.org/10.1080/01431161.2018.1508922
Parrot Sequoia [WWW Document], n.d. URL https://www.parrot.com/en/shop/accessories-spare-parts/other-drones/sequoia-calibration-target (accessed 12.1.21).
Paz-Kagan, T., Silver, M., Panov, N., Karnieli, A., 2019. Multispectral Approach for Identifying Invasive Plant Species Based on Flowering Phenology Characteristics. Remote Sens. 11, 953. https://doi.org/10.3390/rs11080953
Pix4D community [WWW Document], 2022. URL https://community.pix4d.com/t/interpretation-of-gcps-and-cps-errors-to-assess-the-quality-of-a-project/6451
Processing steps - Support [WWW Document], 2022. URL https://support.pix4d.com/hc/en-us/articles/115002472186-Processing-steps (accessed 6.15.22).
Prošek, J., Šímová, P., 2019a. UAV for mapping shrubland vegetation: Does fusion of spectral and vertical information derived from a single sensor increase the classification accuracy? Int. J. Appl. Earth Obs. Geoinf. 75, 151–162. https://doi.org/10.1016/j.jag.2018.10.009
Prošek, J., Šímová, P., 2019b. UAV for mapping shrubland vegetation: Does fusion of spectral and vertical information derived from a single sensor increase the classification accuracy? Int. J. Appl. Earth Obs. Geoinf. 75, 151–162. https://doi.org/10.1016/j.jag.2018.10.009
Radoglou-Grammatikis, P., Sarigiannidis, P., Lagkas, T., Moscholios, I., 2020. A compilation of UAV applications for precision agriculture. Comput. Networks 172, 107148. https://doi.org/10.1016/j.comnet.2020.107148
Rajendra, Y.D., Mehrotra, S.C., Kale, K. V., Manza, R.R., Dhumal, R.K., Nagne, A.D., Vibhute, A.D., 2014. Evaluation of partially overlapping 3D point cloud's registration by using ICP variant and cloudcompare. Int. Arch. Photogramm. Remote Sens. Spat. Inf. Sci. - ISPRS Arch. XL–8, 891–897. https://doi.org/10.5194/isprsarchives-XL-8-891-2014
Räsänen, A., Virtanen, T., 2019. Data and resolution requirements in mapping vegetation in spatially heterogeneous landscapes. Remote Sens. Environ. 230, 111207. https://doi.org/10.1016/j.rse.2019.05.026

Rewilding Europe [WWW Document], n.d. . Gt. Côa Val. URL https://rewildingeurope.com/areas/greater-coa-valley/ (accessed 11.26.21).
Sanz-Ablanedo, E., Chandler, J.H., Rodríguez-Pérez, J.R., Ordóñez, C., 2018. Accuracy of Unmanned Aerial Vehicle (UAV) and SfM Photogrammetry Survey as a Function of the Number and Location of Ground Control Points Used. Remote Sens. 2018, Vol. 10, Page 1606 10, 1606. https://doi.org/10.3390/RS10101606
Schonberger, J.L., Frahm, J.M., 2016. Structure-from-Motion Revisited. Proc. IEEE Comput. Soc. Conf. Comput. Vis. Pattern Recognit. 2016-December, 4104–4113. https://doi.org/10.1109/CVPR.2016.445
Schwind, M., Starek, M., 2017. Structure-from-motion photogrammetry. GIM Int. 31, 36–39.
Seifert, E., Seifert, S., Vogt, H., Drew, D., van Aardt, J., Kunneke, A., Seifert, T., 2019. Influence of drone altitude, image overlap, and optical sensor resolution on multi-view reconstruction of forest images. Remote Sens. 11, 1252. https://doi.org/10.3390/rs11101252
Sharma, J.B., 2019. Applications of small unmanned aircraft systems: Best practices and case studies, 1st ed. CRC Press, Boca Raton. https://doi.org/https://doi.org/10.1201/9780429244117
Sharrock, S., Jackson, P.W., 2017. Plant conservation and the sustainable development goals: A policy paper prepared for the global partnership for plant conservation. Ann. Missouri Bot. Gard. 102, 290–302. https://doi.org/10.3417/D-16-00004A
Statistics, S., Assessment, A., n.d. Tutorial - Sample Statistics and Accuracy Assessment.
Strong, C.J., Burnside, N.G., Llewellyn, D., 2017. The potential of small-Unmanned Aircraft Systems for the rapid detection of threatened unimproved grassland communities using an Enhanced Normalized Difference Vegetation Index. PLoS One 12, 1–16. https://doi.org/10.1371/journal.pone.0186193
Tay, J.Y.L., Erfmeier, A., Kalwij, J.M., 2018. Reaching new heights: can drones replace current methods to study plant population dynamics? Plant Ecol. 219, 1139–1150. https://doi.org/10.1007/s11258-018-0865-8
Thomas, D., 2019. The Greater Côa Valley: how rural architecture can help build a future for nature [WWW Document]. endangeredlandscapes.org. URL https://www.endangeredlandscapes.org/the-greater-coa-valley-how-rural-architecture-can-help-build-a-future-for-nature/ (accessed 11.22.21).
UgCS [WWW Document], n.d. URL https://www.ugcs.com/ (accessed 6.17.22).
Ventura, D., Bonifazi, A., Gravina, M.F., Belluscio, A., Ardizzone, G., 2018. Mapping and classification of ecologically sensitive marine habitats using unmanned aerial vehicle (UAV) imagery and Object-Based Image Analysis (OBIA). Remote Sens. 10, 1–23. https://doi.org/10.3390/rs10091331
Xie, Y., Sha, Z., Yu, M., 2008. Remote sensing imagery in vegetation mapping: a review. J. Plant Ecol. 1, 9–23. https://doi.org/10.1093/jpe/rtm005
Yang, K., Zhang, H., Wang, F., Lai, R., 2022. Extraction of Broad-Leaved Tree Crown Based on UAV Visible Images and OBIA-RF Model: A Case Study for Chinese Olive Trees. Remote Sens. 14, 2469. https://doi.org/10.3390/rs14102469
Yang, X., 2007. Integrated use of remote sensing and geographic information systems in riparian vegetation delineation and mapping. http://dx.doi.org/10.1080/01431160600726763 28, 353–370. https://doi.org/10.1080/01431160600726763
Zhou, R., Yang, C., Li, E., Cai, X., Yang, J., Xia, Y., 2021. Object-based wetland vegetation classification using multi-feature selection of unoccupied aerial vehicle rgb imagery. Remote Sens. 13. https://doi.org/10.3390/rs13234910
Zilhão, J., Aubry, T., Carvalho, A.F., Baptista, A.M., Gomes, M. V., Meireles, J., 1997. The Rock Art of the Côa Valley (Portugal) and its Archaeological Context: First Results of Current Research. J. Eur. Archaeol. 5, 7–49. https://doi.org/10.1179/096576697800703601

7. APPENDIX

Annex 1

Parameters used for image acquisition in Vale Carapito and Ermo das Águias (used by Rewilding Portugal)

Flight Parameters	**Vale Carapito**	**Ermo das Águias**
Flying height	150m	Between 30-86m
Flying speed	14m/s	14m/s
Forward overlap	65%	85%
Side overlap	65%	65-75%
Ground sampling distance	3.90cm	2.0cm

The flight in Ermo das Águias covered a grazing area of 312hectares and was sampled into seven plots of 7hecatres. In comparison, Vale Carapito covered a grazing area of 54 hectares, sampled into five plots.

Annex 2: Flight plans of Vale Carapito (Plot 5) and Ermo das Águias (Plot 5)

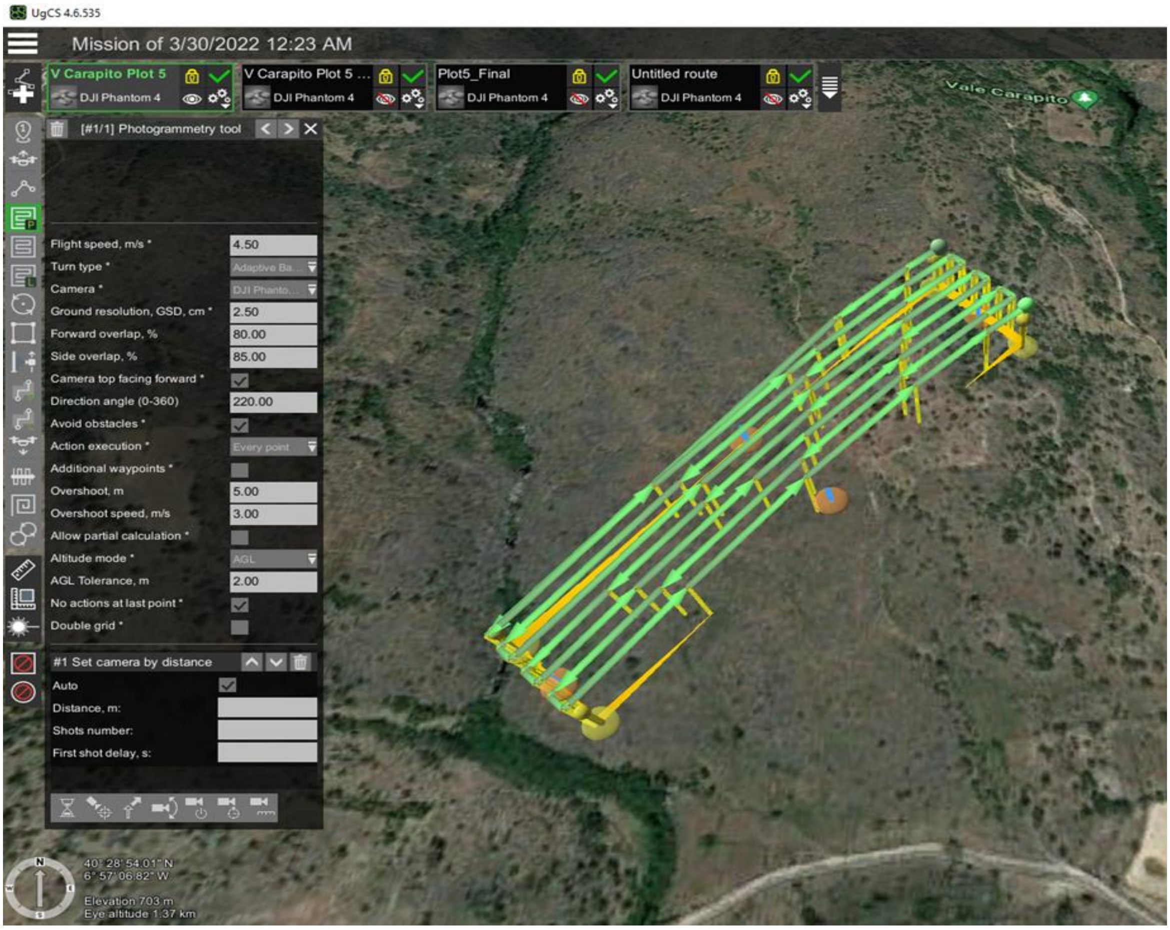

Annex 3

Distribution of GCP (blue marks) and the images (red dots) in Vale Carapito (map view)

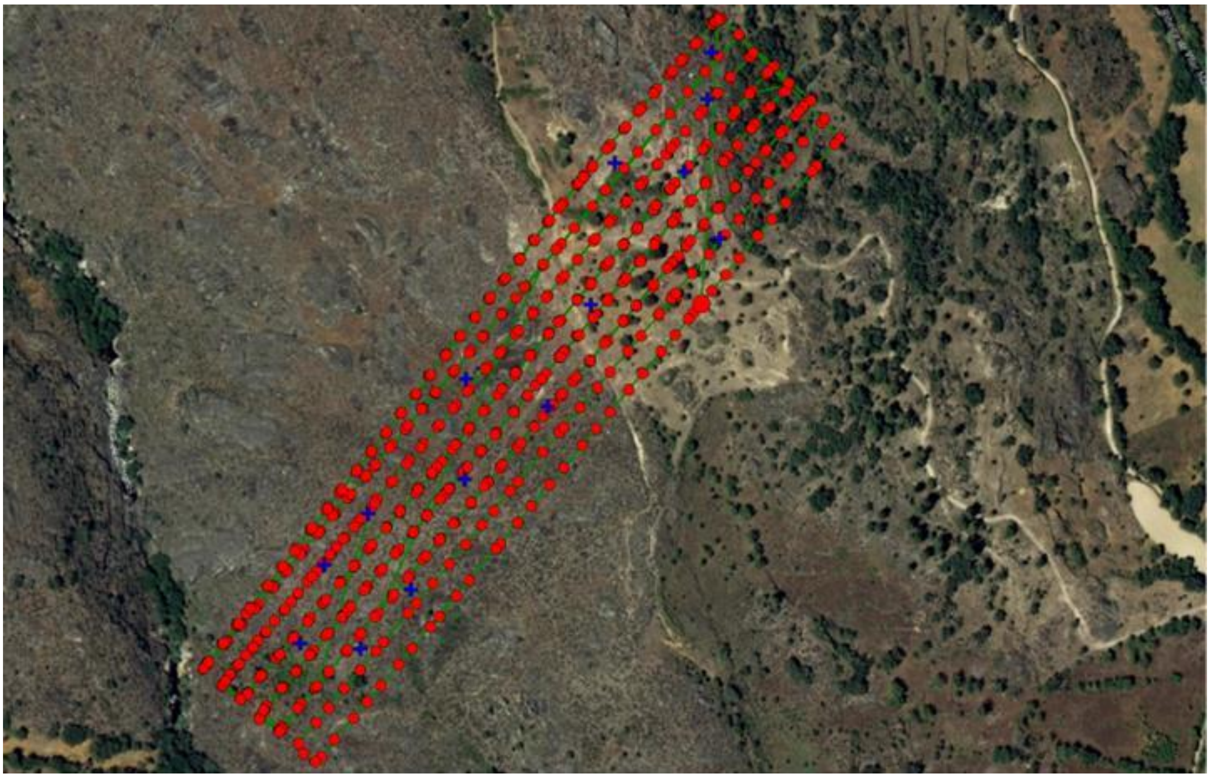

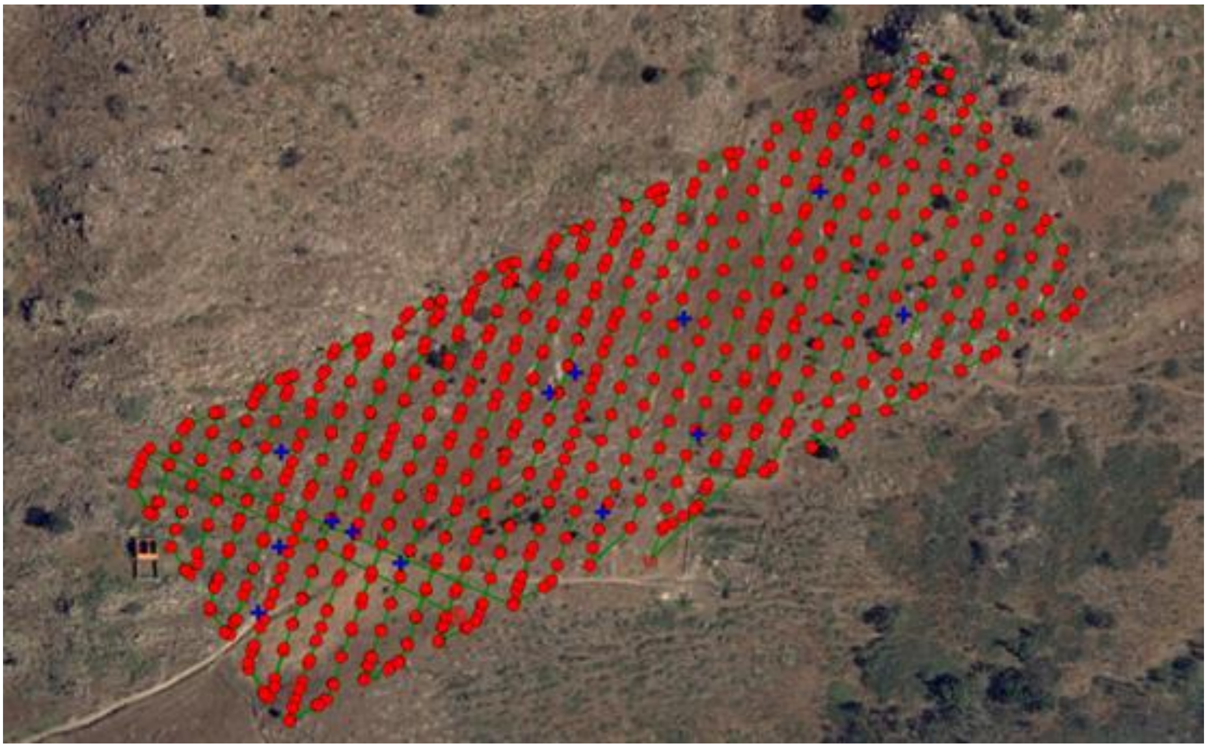

Distribution of GCP (blue marks) and the images (red dots) in Ermo das Águias (map view)

Annex 4:

Overlap of UAV-RGB JPEG, TIFF, and Multispectral images for winter.

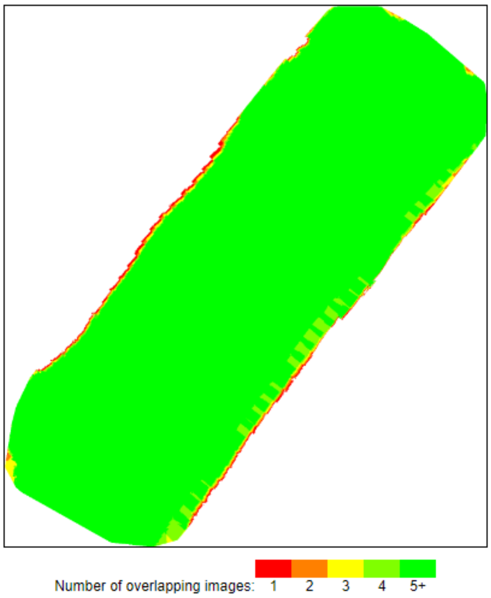

UAV-RGB JPEG

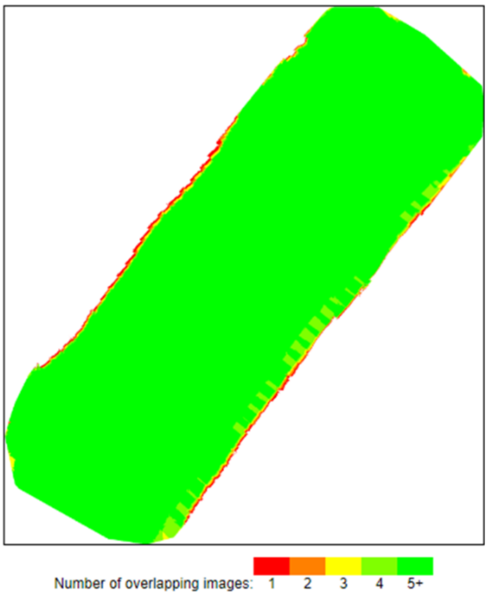

UAV-RGB JPEG (without GCP)

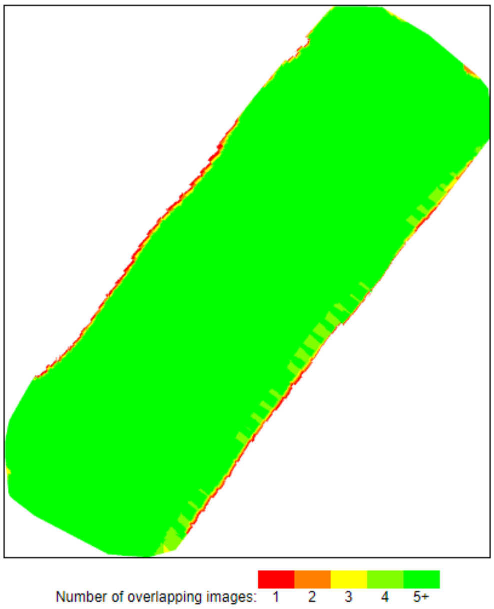

UAV-RGB TIFF

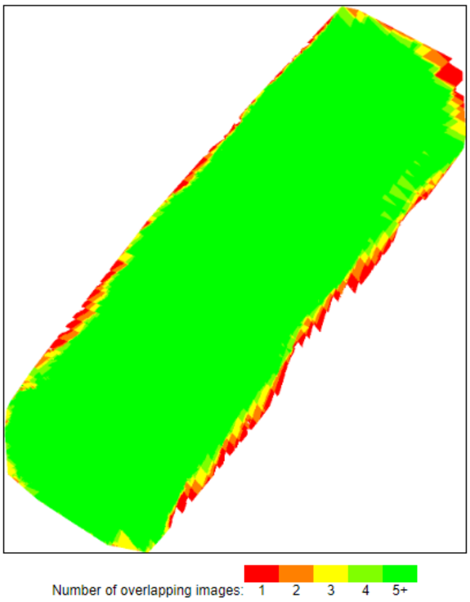

UAV-MS

Summary of quality reports from SfM processing using Pix4D mapper (for Ermo das Águias)

Features	UAV-RGB(TIFF)		
Number of images	677 (100% calibrated)		
Number of GCP	9		
Mean Reprojection Error	0.186		
GCP RMSE (m)	0.043		
RMSE (X, Y, Z)	0.04	0.02	0.06
Checkpoint RMSE (m)	0.12	0.04	0.2
Coordinate system	WGS 84/UTM zone 29N		
Point Cloud average density (per m^3)	1135.83		

Overlap of UAV-RGB TIFF images computed for each pixel of the orthomosaic.

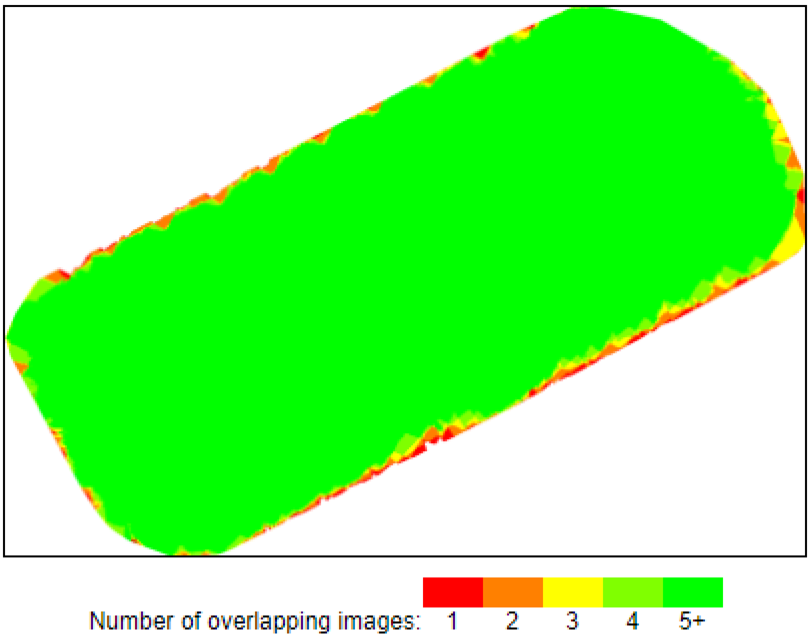

Annex 5: Vegetation indices used for RGB imagery in eCognition

Spectral Vegetation Indices (RGB)	Equation	Reference
GLI (Green Leaf Index)	$(G^2-R-B)/(G^2+R+B)$	(Lussem et al., 2018)
NGBDI (Normalized Green Blue Difference Index)	(G-B)/(G+B)	(Du and Noguchi, 2017)
RGBVI (Red Green Blue Vegetation Index)	$(G^2-R*B)/(G^2+R*B)$	(Bendig et al., 2015; García-Fernández et al., 2021)
MGVRI (Modified Green Red Vegetation Index)	$(G^2-R^2)/(G^2+R^2)$	(Bendig et al., 2015)
NDSI (Normalized Difference Soil Index)	(R-G)/(R+G)	(F. Chen et al., 2021)
GRVI (Green-Red Vegetation Index)	(G-R)/(G+R)	(Bendig et al., 2015)

Vegetation indices used for MS imagery in eCognition

Spectral Vegetation Indices	Equation	Reference
GCI (Green chlorophyll Index)	((NIR/G)-1)	
NDVI (Normalized Difference Vegetation Index)	(NIR-R)/(NIR+R)	(Ashapure et al., 2019; Fuentes-Peailillo et al., 2019)
NDRE (Normalized Difference Red edge Index)	(NIR - RE)/ (NIR + RE)	(Macintyre et al., 2020)
MGVRI (Modified Green Red Vegetation Index)	$(G^2-R^2)/(G^2+R^2)$	(Bendig et al., 2015)
SAVI (Soil-Adjusted Vegetation Index)	((NIR-R)/(NIR+R+L)) * (1+L)	(Huete, 1988)
GRVI (Green-Red Vegetation Index)	(G-R)/(G+R)	(García-Fernández et al., 2021)
NDWI (Normalized Difference Water Index)	(G-NIR)/(G+NIR)	(F. Chen et al., 2021)

Annex 6:

Confusion matrix generated with 105 training samples

Confusion Matrix (JPEG)								
User class	**Grass**	**Bracken**	**Shrubs**	**Rock**	**Trees**	**Bare soil**	**Lichens**	**Sum**
Grass	19	2	3	0	1	10	0	35
Bracken	0	4	2	3	0	0	1	10
Shrubs	2	10	25	3	6	0	3	49
Rock	12	6	9	29	0	2	7	65
Trees	0	1	0	1	39	0	0	41
Bare soil	0	0	0	0	0	2	0	2
Lichens	5	0	2	1	0	0	18	26
Sum	38	23	41	37	46	14	29	
Accuracy								
Producer	0.5	0.18	0.61	0.78	0.85	0.14	0.62	
User	0.54	0.4	0.51	0.44	0.95	1	0.69	
Overall Accuracy: 59.65% **Kappa: 0.516**								

Confusion Matrix (TIFF)								
User class	**Grass**	**Bracken**	**Shrubs**	**Rock**	**Trees**	**Bare soil**	**Lichens**	**Sum**
Grass	44	7	26	4	14	28	1	124
Bracken	6	5	9	9	0	0	2	31
Shrubs	13	14	58	15	14	1	4	119
Rock	7	5	9	28	1	2	14	66
Trees	0	2	1	3	63	0	0	69
Bare soil	0	0	0	1	0	6	1	8
Lichens	9	0	5	8	3	1	24	50
Sum	79	33	108	68	95	38	46	
Accuracy								
Producer	0.55	0.15	0.54	0.41	0.66	0.16	0.52	
User	0.35	0.16	0.48	0.42	0.91	0.75	0.48	
Overall Accuracy: 48.82% **Kappa: 0.383**								

Annex 7

Representation of the plot in cloudcompare using point clouds(with GCP & without GCP) and the cloud-to-cloud absolute distance range.

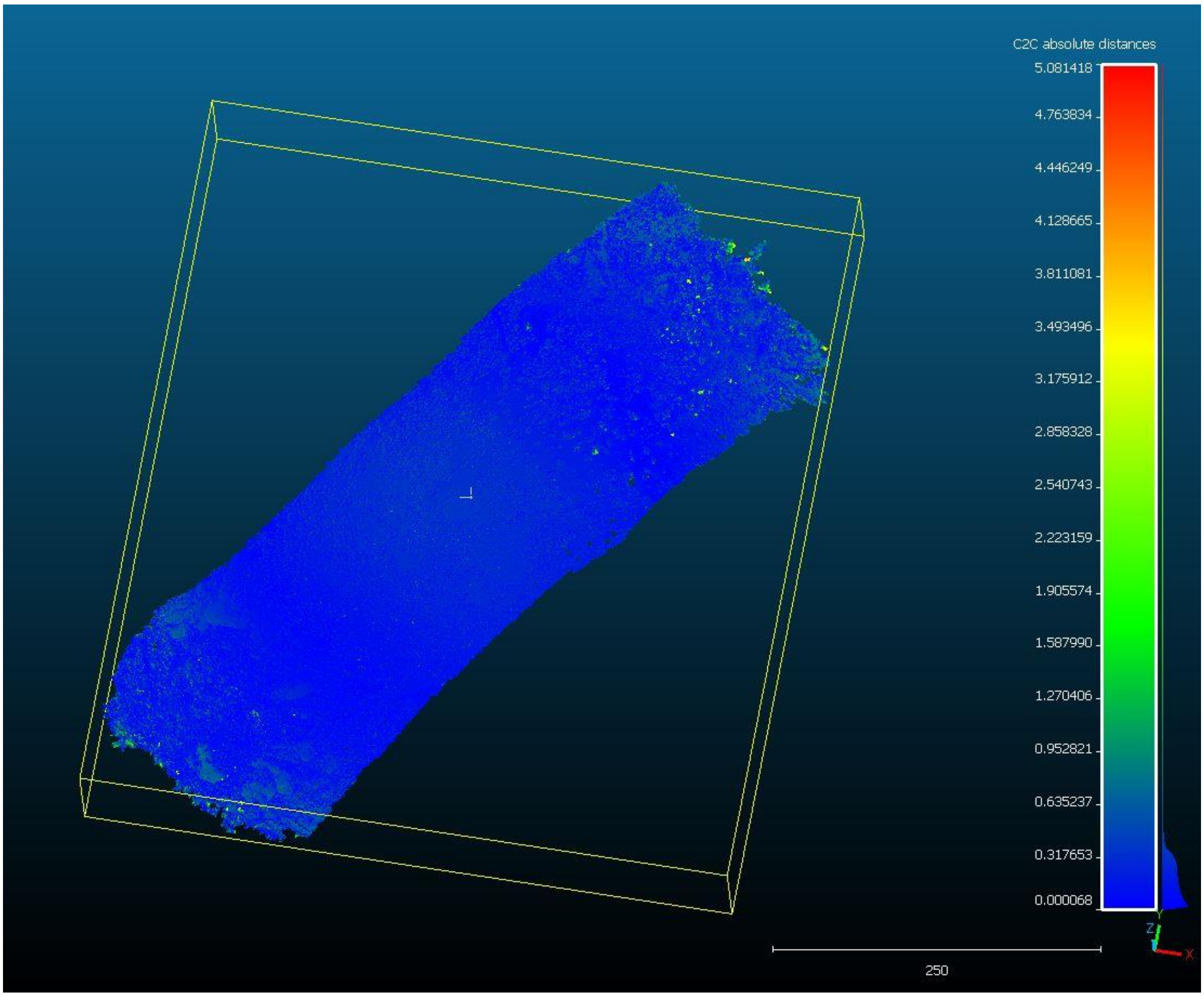

Residuals after ICP registration

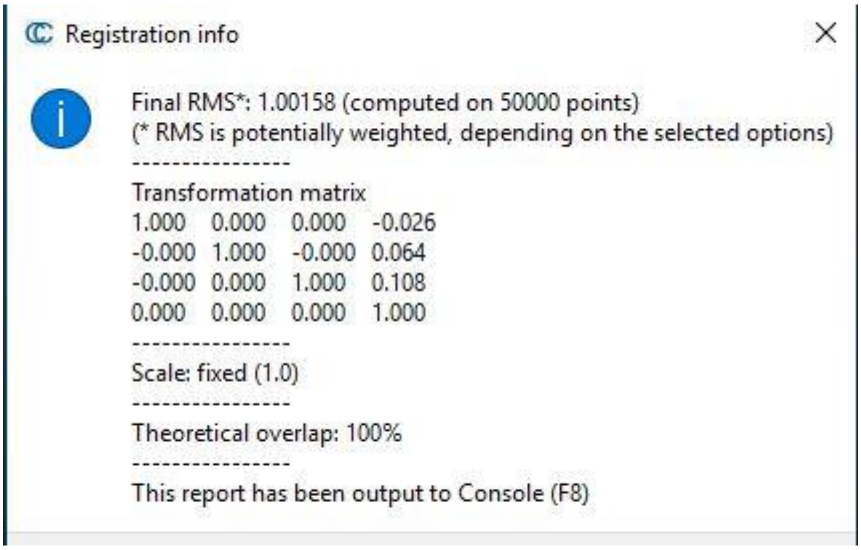

Registration info

Final RMS*: 1.00158 (computed on 50000 points)
(* RMS is potentially weighted, depending on the selected options)

Transformation matrix

1.000	0.000	0.000	-0.026
-0.000	1.000	-0.000	0.064
-0.000	0.000	1.000	0.108
0.000	0.000	0.000	1.000

Scale: fixed (1.0)

Theoretical overlap: 100%

This report has been output to Console (F8)